THIRTEENTH EUROPEAN ROTORCRAFT FORUM

79

Paper No 95

THE IDENTIFICATION OF REDUCED ORDER MODELS OF HELICOPTER BEHAVIOUR FOR HANDLING QUALITIES STUDIES

by

S. S. Houston
Lt Cdr R. I. Horton, RN

Procurement Executive, Ministry of Defence
Royal Aircraft Establishment
Flight Systems Department
Bedford MK41 6AE
England

September 8-11, 1987
Arles, France

ASSOCIATION AERONAUTIQUE ET ASTRONAUTIQUE DE FRANCE

1 INTRODUCTION

Future rotorcraft will be required to demonstrate compliance with emerging handling qualities criteria[1,2,3], to quantify the ease and precision with which they can be flown to fulfil a given task. The use of accurate mathematical models should ease the design process, allowing optimisation of the helicopter before the expensive and time-consuming phase of flight-testing. This, together with a comprehensive, accurate and applicable handling qualities database should allow the designer to tailor a new vehicle's handling qualities to potential tasks before first flight. The required level of model accuracy however, is likely to result in increased model complexity and order, generally to the extent that a simple, interpretative understanding of the dynamic characteristics of concern is no longer available. In addition, the current handling qualities database is sparse and incomplete. This Paper addresses the dual aims of model simplification and verification. The results are placed in the context of the proposed revisions[1,2] to the MIL-H-8501A handling qualities specification. Broadly, the use of the equivalent systems concept as an analytical tool for understanding complex helicopter mathematical modelling problems is examined. Corresponding models are derived from open-loop flight-testing, both to verify the theoretical model (in this case RAE's 12 degree-of-freedom (DOF) HELISTAB model[4]), as an equivalent system, and to provide simple, accurate models of the helicopter for off-line simulation studies. A demanding pilot-in-the-loop tracking task has been developed to generate a database of handling qualities results, which is used with the vehicle models to explore the applicability of proposed bandwidth criteria, Fig 1, specified in the proposed revisions of MIL-H-8501A. The analysis has concentrated on the short-period pitch response of a typical articulated rotor helicopter, the Puma, Fig 2. Additional complementary material from the recently initiated flight research program on the RAE Bedford Lynx helicopter, Fig 3, is also included to highlight differences in the flight dynamic behaviour of hingeless and articulated rotor helicopters.

2 SYNTHESIS OF REDUCED ORDER MODELS

The need to model rotorcraft in reduced form is particularly acute since, quite apart from facets of their behaviour such as non-linearity, the vehicle's response to disturbances is complex, multi-modal, cross-coupled and either inherently unstable (in unaugmented form), or governed to a significant extent by a sophisticated stabilisation system. All of these features cloud insight into a fundamental understanding of flight behaviour. An additional complicating factor is that to extend the frequency range over which a helicopter flight mechanics model is representative, rotor flapping dynamics need to be incorporated. As well as increased model order and hence complexity (which will therefore reduce any insight even further) this results in stability and control derivatives (such as M_q , pitch rate damping and $M_{\theta 1s}$, pitch moment per unit longitudinal cyclic control input) losing their conventional meaning. The M_q and $M_{\theta 1s}$ derivatives for example, still contribute to pitch damping and control moment, but tell only part of the overall story. Due attention has to be paid to flapping per unit control, and moment per unit flapping derivatives. It is one of the modelling objectives of this Paper to show that such high order mathematical descriptions of conventional single main and tail rotor helicopters, as well as models derived from flight-test, can be reduced or equivalenced by models of in this case, the conventional form for short-period pitch motion. In doing so, the traditional interpretation placed on stability and control parameters by flight dynamicists and test pilots alike, is restored.

The model reduction, or in the case of the flight-derived models, parameterisation, is accomplished in the frequency domain by choosing the parameters in the reduced order model structure such that this model's frequency response matches (or equivalences) that of the full system or flight result. This matching is performed numerically as a least-squares minimisation problem. If

$$G_{xy}(s) = G'_{xy}(s)F(s) \tag{1}$$

then the reduced order model frequency response $G'_{xy}(s)$ identically matches that of the full system or flight result $G_{xy}(s)$ if

$$\left| F(s) \right| = 1 \; ; \; \angle F(s) = 0 \tag{2}$$

over all $\omega : \omega_1 < \omega < \omega_m$. Substituting $i\omega$ for s , equation (1) can be rewritten as

$$\left| F(\omega) \right| = \frac{\left| G_{xy}(\omega) \right|}{\left| G'_{xy}(\omega) \right|} \; , \; \angle F(\omega) = \angle G_{xy}(\omega) - \angle G'_{xy}(\omega) \tag{3}$$

and defining the cost function to be minimized as

$$J = \sum_{\omega=\omega_1}^{\omega=\omega_m} \left[W_g \left(\left| F(\omega) \right| - 1 \right)^2 + W_p \left(\angle F(\omega) \right)^2 \right] \tag{4}$$

then it can be seen that as $J \to 0$ (0 being the minimum that a least-squares minimisation seeks to achieve)

$$\left.\begin{array}{l} |F(\omega)| - 1 \to 0 \Rightarrow |F(\omega)| \to 1 \Rightarrow |G'_{xy}(\omega)| \to |G_{xy}(\omega)| \\ \angle F(\omega) \to 0 \Rightarrow \angle G'_{xy}(\omega) \to \angle G_{xy}(\omega) \end{array}\right\}. \tag{5}$$

Weighting terms W_g and W_p are included so that some control can be exercised over solutions with significant mismatch between actual and equivalent frequency responses. In this Paper, incidence and pitch rate frequency responses are simultaneously matched, since if the incidence and pitch rate responses can be modelled in 'classical' short-period form, then their transfer functions share a common denominator. Simultaneous equivalencing of j frequency responses renders equation (4) in vector form, viz

$$J = \sum_{\omega=\omega_1}^{\omega=\omega_n} \left[\underline{W}_g \left(|\underline{F}(\omega)| - 1\right)^2 + \underline{W}_p \left(\angle \underline{F}(\omega)\right)^2\right] \tag{6}$$

where $\underline{W}_g$ *and* $\underline{W}_p$ *are j-element row vectors of weights, and* $\underline{F}$ is a j-element column vector of the mismatch frequency responses. For theoretical models such as RAE's HELISTAB, which can be represented in linearised state-space form as

$$\dot{x} = Ax + Bu \tag{7}$$

the frequency response matrix $\underline{G}$, containing the relevant elements $\underline{G}_{xy}$ is calculated explicity from

$$\left.\begin{array}{l} \mathrm{Re}(\underline{G}) = -A(A^2 + I\omega^2)^{-1}B \\ \mathrm{Im}(\underline{G}) = -\omega(A^2 + I\omega^2)^{-1}B \end{array}\right\}. \tag{8}$$

Details associated with the calculation of equivalent systems by the method outlined above are contained in Ref 5. In particular, models given by equation (7) that possess unstable modes can still be equivalenced by frequency response matching: a modal decomposition technique is presented in Ref 5 that allows the model to be split into a sum of a stable modes subsystem and an unstable modes subsystem, even for strongly coupled systems. The equivalencing is then performed on the former, the resulting reduced model being recombined with the unstable modes subsystem. Resulting models may typically be of 3rd or 4th order, but this is considerably more manageable than a 14th order, 12 DOF model. In any case, if the resulting model is to be used to predict transient response to control inputs, the modal decomposition can be used to highlight the contribution of the unstable modes to the total response over the time range of interest. Judgement can then be used to decide if the unstable modes make a significant enough contribution to the response to merit inclusion in the reduced model. None of the 12 DOF Puma models reduced in this Paper possess any unstable modes.

Frequency responses from flight data are obtained using time series analysis techniques. It is not proposed in this Paper to explore the detail of this approach for system identification; readers unfamiliar with this field are referred to texts such as Refs 6 and 7, which provide both a good introduction to this area, as well as a comprehensive coverage of it. In outline however, power spectral density functions of the input and output measurements, $\hat{G}_{xx}(\omega)$ and $\hat{G}_{yy}(\omega)$ respectively, together with the complex-valued cross-spectral function

$$\hat{G}_{xy}(\omega) = c(\omega) + id(\omega)$$

are used to calculate the input-output coherency function

$$\gamma^2_{xy}(\omega) = \frac{|\hat{G}_{xy}(\omega)|^2}{\hat{G}_{xx}(\omega)\hat{G}_{yy}(\omega)} \tag{10}$$

which is important as it gives a direct quantitative measure of the frequency range across which the derived model is linear. System gain and phase are given respectively by

$$|\hat{H}_{xy}(\omega)| = \frac{|\hat{G}_{xy}(\omega)|}{\hat{G}_{xx}(\omega)}, \quad \angle\hat{H}_{xy}(\omega) = \cos^{-1}\left(\frac{c(\omega)}{|\hat{G}_{xy}(\omega)|}\right). \tag{11}$$

There is considerable scope for the use of engineering judgement in the application of time series analysis methods, to vary the appearance of the resulting frequency response, and its apparent linearity (the coherency function). The iterative approach taken to obtain the results presented in this Paper is outlined in Ref 8. The widely-published work of Tischler[9-11] serves to emphasise the efficacy of time series analysis methods for identifying XV-15 tilt-rotor aircraft response characteristics. More recently, their applicability to conventional single main and tail rotor helicopters has also been demonstrated[8,12].

Now the conventional form for the short-period approximation model structure is given in state-space form as

$$\begin{bmatrix} \dot{\alpha} \\ \dot{q} \end{bmatrix} = \begin{bmatrix} Z_\alpha & Z_q \\ M_\alpha & M_q \end{bmatrix} \begin{bmatrix} \alpha \\ q \end{bmatrix} + \begin{bmatrix} Z_{\eta 1s} \\ M_{\eta 1s} \end{bmatrix} \eta_{1s} \quad . \tag{12}$$

In transfer function form, this model structure gives

$$\frac{\alpha}{\eta_{1s}} = Z_{\eta_{1s}} \frac{s - \delta_\alpha}{s^2 + 2\zeta\omega_n s + \omega_n^2}, \qquad \frac{q}{\eta_{1s}} = M_{\eta_{1s}} \frac{s - \delta_q}{s^2 + 2\zeta\omega_n s + \omega_n^2} \tag{13}$$

and the normal acceleration transfer function is (since $n_g = V_f q - \dot{w}$, and $w = V_f \alpha$)

$$\frac{n}{\eta_{1s}} = Z_n \frac{s^2 + a_n s + b_n}{s^2 + 2\zeta\omega_n s + \omega_n^2} \quad . \tag{14}$$

To each transfer function is added a pure time delay term $e^{-\tau s}$, to capture high frequency phase effects such as those due to actuation and rotor flapping dynamics. The model structures given in equations (13) and (14), together with their respective delay terms, form the G'_{xy} used in the equivalencing procedure described previously.

3 REDUCTION OF THEORETICAL MODELS

Fig 4 presents a comparison of short-period motion variable frequency responses calculated for a 12 DOF model of the Puma at 60 kn, with those of the reduced order model synthesised as described in the previous section. The matching has been performed over the frequency interval of 0.1-1.0 Hz (0.628-6.28 rad/s), and it can be seen that the equivalent, or reduced model, is an excellent match in this frequency range. Gain and phase characteristics are both accurately represented in the reduction; in particular, the equivalent system captures the non-minimum phase characteristic of the vertical velocity (incidence) response to longitudinal cyclic, and the 'roll-off' at high frequency in the pitch rate response, caused by the rotor flapping dynamics. The applicability of this model for predicting short-period transient response to multi-step inputs of longitudinal cyclic is shown in Fig 5. The doublet inputs and their corresponding frequency content are shown in Fig 5a. It is clear that the degree of fidelity offered by the reduced model is more than adequate for capturing the transient response to cyclic inputs given by the 12 DOF description. The use of the equivalent delay term allows the reduced order model to capture the lagged effect on pitch rate response caused by the incorporation of 2nd order flapping dynamics in the 12 DOF model.

Figs 6 and 7 illustrate the corresponding results to Figs 4 and 5 for the 120 kn flight condition, and confirm the applicability of the model reduction for matching the 12 DOF model frequency response characteristics, and time domain transient response. Note from Fig 6 however, an additional feature of the helicopter's response around 0.16 Hz (1.0 rad/s): the resonant peak in each gain response, and corresponding changes in the phase responses, occurs as a consequence of the dutch roll mode (which cross-couples into the pitching response in the Puma) becoming increasingly lightly damped as speed is increased. This multi-modal characteristic of the helicopter's response is also present in the 60 kn result, but the dutch roll mode is much more heavily damped at this speed. The result is that the total frequency response looks much more like a 2nd order system, and hence the model structure given by equation (13) can accurately mimic the 12 DOF model frequency response. For the 120 kn model, a 4th order model structure would need to be used to capture the detail effects of the lightly damped dutch roll mode around 1 rad/s. However, the reduced, equivalent model derived is the 'best' (in a least-squares sense) 2nd order approximation, and the time domain 'verification' results shown in Fig 7 indicate that the resulting low frequency mismatch is not significant enough to adversely effect the predictive quality of the equivalent.

The modal decomposition technique described in the previous section as a means of splitting unstable systems into stable and unstable parts, has been used to separate the mode recognisable as being of classical short-period form, from the total system frequency response, Fig 8. This has been done to emphasise that the model reduction by equivalencing is not trivial, in the sense that a 2nd order model structure has been used to match a system that is intrinsically 2nd order in nature. It is quite obvious that the short-period mode contributes only partly to the total response in each of the states that are considered to characterise

short-period pitching motion. This figure emphasises that the short-period pitch response to longitudinal cyclic inputs is truly multi-modal in nature, and therefore the reduced order models produced are indeed equivalent systems. The model parameter set

$$\{\delta_w \ \delta_q \ \zeta \ \omega_n \ \tau_w \ \tau_q \ Z_{\theta_{1s}} \ M_{\theta_{1s}}\}$$

and resulting stability derivatives

$$[Z_w \ Z_q \ M_w \ M_q]$$

are therefore equivalent or effective parameters and derivatives only, and do not necessarily equate to corresponding stability and control derivatives to be found in the full equations of motion. The implications of this fact are further discussed in section 8 of the Paper.

Reduced order models of normal acceleration response to cyclic inputs, in the form of equation (14), are compared with the corresponding 12 DOF model frequency responses for the 60 and 120 kn flight conditions in Figs 9 and 10 respectively. The quality of each match is comparable with those obtained for the vertical velocity and pitch rate responses, and once again the lightly damped dutch roll mode manifests itself quite obviously in the 120 kn case. Nonetheless, the equivalent systems accurately capture the form of each 12 DOF model normal acceleration frequency response, including the trough in gain around 0.5 Hz (3.0 rad/s), and the accompanying rapid change in phase. This characteristic is caused by the two contributions to normal acceleration, namely centripetal (given by V_{rq}) and translational ($\dot{w}$) being of similar magnitude, but around 180° out of phase. The equivalent systems can also be seen to accurately model the transient response to a 2 s period doublet input, Fig 11, at both 60 and 120 kn.

The fact that the model structures given by equations (13) and (14) can be used to capture short-period pitch and normal acceleration response characteristics, indicates that these motions manifest themselves in a classical form. This is despite the fact that the response is multi-modal in nature, with longitudinal components of the dutch roll mode contributing substantially to the short-period pitch motion.

4 DERIVATION OF MODELS FROM FLIGHT EXPERIMENTS

This section highlights some results obtained in the derivation of models from flight, that correspond to those derived theoretically. This is for the purposes of verifying the theoretical 12 DOF models, as will be described in section 5. In addition, models are derived from data obtained when the Puma was flown with the augmentation system engaged. This is to explore the applicability of model structures given by equations (13) and (14) for characterising short-period response with the augmentation system engaged, since this contributes nonlinearity (as will be shown), increases the complexity of the aircraft behaviour and also increases the order of the response to control inputs. Models of the Lynx helicopter are also derived. Table 1 summarises flight and aircraft condition test points for which models have been synthesised.

4.1 Aircraft description and flight test technique

The Puma, Fig 2, has been the principal flight research helicopter at RAE Bedford for many years, and although an early development batch aircraft, is in most respects identical to the variant currently operated by the RAF and French ALAT. The RAE vehicle does however, have metal rather than composite main rotor blades, which gives the rotor lower solidity than current production counterparts. Blade flap inertia is additionally a few percent more than the composite blade, although flapping hinge offset remains the same as production aircraft at 3.8% of rotor radius. The aircraft is powered by two Turmo III C4 turboshafts, but lacks the polyvalent air intake filters fitted to many Pumas, and which are known to have some impact on the lateral-directional dynamics. Tests were flown with the fully retractable tricycle landing gear in the retracted position. The helicopter is fully instrumented with air data sensors, two gyro and accelerometer packs, blade root motion sensors and a set of health monitoring strain gauges. Ballast trays are fitted forward and aft of the datum centre-of-mass location, each capable of carrying over 500 kg of ballast. The stability augmentation system fitted to the helicopter provides rate damping in pitch, roll and yaw, with attitude hold in pitch and roll, heading and height hold, and turn coordination; it is nonetheless a low-gain, limited authority system.

The Lynx, Fig 3, forms the successor to the Puma as RAE Bedford's flight research helicopter. This aircraft has a hingeless main rotor (in flap and lag degrees of freedom), giving an equivalent flapping hinge offset of 13%. The helicopter is powered by Gem Mk 203 turboshafts, and having only recently commenced experimental flying, possesses only a basic instrumentation fit. The aircraft is fitted with automatic stabilisation equipment and a Computer Acceleration Control (CAC) device. The former device utilises rate and attitude information in pitch, roll and yaw for stabilisation and attitude hold, provides height hold through collective and heading hold through the tail rotor. The latter device utilises normal acceleration signals driving the collective for additional pitch stabilisation, and a lateral acceleration signal driving the tail rotor for additional yaw stabilisation.

The test technique involved the pilot establishing the aircraft in a steady trim at the desired test condition, and then performing a variable frequency quasi-sinusoidal control input using the longitudinal cyclic stick, all other controls remaining fixed. This technique has been widely reported in the literature as having been applied to the testing of several different types of rotorcraft[8-12]. The flight test observer calls timings to the pilot to establish the 'shape' of the resulting input, and the pilot can adjust input size so that perturbations from

trim remain within a prescribed range. The nominal peak cycle frequency is 2 Hz (12.5 rad/s), although observer counting stops after the input with a 4 s (0.25 Hz) period, since it has been found that the high levels of concentration required by the pilot at frequencies higher than this, can otherwise be disrupted. The literature indicates that outside RAE, it is established practice to choose the lowest cycle period as 24 s (0.04 Hz, 0.26 rad/s), with succeeding cycle periods being half the preceding one. At RAE, the 24 second period is the lowest, but succeeding cycle periods are 4 seconds less than the preceding one. This approach has been developed for two reasons; firstly, halving the input frequency results in a very rapid build-up to the high frequency part of the sweep which the pilot reported as being too fast and degraded the quality of the input at the intermediate-to-high frequencies. Reducing the input cycle period by 4 seconds each time resulted in a much more gradual, controllable and comfortable build-up to the high frequency portion of the sweep. Secondly, the frequency content of these sweeps is such that data from a single sweep can be used in the modelling process. It has been reported elsewhere[9], that concatenation of multiple runs may be required to provide a sufficient number of averages of the data, and acceptable input-output coherency. This has been found not to be the case with the results given in this Paper.

Measurements of control input and aircraft response from a typical sweep (flown at 60 kn with the cg aft of datum) are shown in Fig 12. The frequency content of this particular control input is given in Fig 13, where it can be seen that the spectrum is fairly even over most of the frequency range of concern to the modelling described in this Paper - 0.1-1.0 Hz (0.628-6.28 rad/s). Beyond this up to 1.6 Hz (10 rad/s), the power in the input diminishes only slightly. Not shown in Fig 12 beyond 120 seconds is a return to trim followed by a control doublet input. This is done to provide data for the verification of the model derived from the frequency sweep, with an input type dissimilar to that used in the identification process. Although RAE possesses a broad database of Puma response to multi-step inputs gathered over many years, it has become standard practice to complete each sweep with a doublet input of chosen amplitude and duration. This data is then directly relevant to the vehicle configuration and test conditions.

4.2 Synthesis of flight-derived models

For the purposes of illustration, the modelling of the Puma relevant to the measurements shown in Fig 12 is used as typical of the results obtained with this aircraft. This configuration is one of the augmentation engaged runs. Fig 14a&b shows the incidence and pitch rate to longitudinal cyclic frequency responses derived using time series analysis techniques, together with the relevant input-output coherency functions. The frequency response of the equivalent system fit is also shown on these figures. There are several points worthy of note. Firstly, the form of the frequency responses is very similar to those given by the 12 DOF HELISTAB model; secondly, the equivalent system match is very good over the frequency range of interest, 0.1-1.0 Hz (0.628-6.28 rad/s). Thirdly, the coherency functions show that confidence in the linearity of the incidence model diminishes rapidly below about 0.1 Hz (0.628 rad/s), but is maintained down to about 0.015 Hz (0.09 rad/s) for the pitch rate model. It can be concluded therefore that over the 0.1-1.0 Hz frequency range, the augmented Puma exhibits 'classical' short-period pitch response to cyclic inputs. Although the flight-derived pitch rate to cyclic frequency response is acceptably linear below 0.1 Hz, the growing mismatch between it and the equivalent system fit indicates that below this frequency, the response characteristics cannot be represented in classical short-period form. Note also from the pitch rate coherency function, the noticeable 'step down' below 0.25 Hz (1.5 rad/s). This feature is found to be common to all Puma configurations flown with augmentation engaged, and is associated with nonlinear behaviour of the augmentation system. This aspect will be returned to in section 6 of the Paper.

The corresponding normal acceleration modelling is shown in Fig 15. Once again, note the quality of the equivalent system match, particularly in gain, and the overall similarity of the frequency response with that of the 12 DOF HELISTAB representation of the Puma. The trough in gain however, is much sharper and steeper than in HELISTAB (as seen in Figs 9 and 10), and associated with it is a relatively broad - over 0.15 Hz (1.0 rad/s) - trough in coherency. The physical reason for the trough in gain and rapid change in phase is given in section 3, the reason for the trough in coherency is a consequence of the response shown by the gain result around 0.5 Hz (3.1 rad/s). The aircraft normal acceleration response at this frequency is negligible and as a result the accelerometer signal is dominated by noise and not by the (otherwise linear) process. This normal acceleration result is explored in Ref 8 where it is demonstrated that use of a higher resolution window can improve the quality of the model. The spectral analysis procedure used to produce Fig 15, while acceptable for pitch rate and incidence models, is not optimised to show the exact shape of the dip in the normal acceleration result. Fig 16 shows the same data analysed using a modified analysis procedure which produces a better definition of the form of the dip.* Note that although the trough in coherency is still sharp and deep, it is much less wide than the result shown in Fig 15 and reaches down to a value of 0.1 instead of 0.0. The frequency response itself is subtly different; the gain trough is not so deep, and the phase response indicates a true non-minimum phase characteristic with crossover at -180° to +180°, unlike the result given in Fig 15, where there is simply a very rapid change in phase, rather like the theoretical model result shown in Figs 9 and 10. Note also that the mismatch in phase is much less at the higher frequencies in Fig 16. Table 2 compares the equivalent model parameters relevant to the results shown in Figs 15 and 16. Although the changes in the parameters are slight, the change in a_n emphasises the different nature of the phase response between the result shown in Fig 15 and that shown in Fig 16, the negative value being indicative of equivalent system zeros in the right-half (unstable) plane of the root locus, as opposed to the left-half (stable). The models derived from results obtained with the latter, optimised window, are used as the definitive characterisations of Puma short-period normal acceleration.

---

* Fig 15 produced using Parzen (cosine) window with bandwidth of 0.002414 Hz
Fig 16 produced using Daniell (rectangular) window with bandwidth of 0.000977 Hz

Examples of model verification in the time domain, using doublet inputs, is shown in Fig 17a-c. Such verification is important to establish the correctness of the synthesised models, and their appropriateness and range of applicability for use in an offline simulation. It can be seen for the examples shown in Fig 17, that the models more than adequately capture the response measured in flight. Although these cases are typical of that found for the other models, those shown in Fig 17 have been chosen because they can be used collectively to explore the linearity of the Puma's response with respect to input magnitude, direction, rate of application, frequency content and aircraft configuration. The examples shown cover all of these aspects, and only Fig 17c reveals some evidence of non-linearity. This case is for flight at 100 kn, mid centre-of-mass location and augmentation disengaged. Although the model accurately predicts the incidence response, and the overall form and salient features of the pitch rate and normal acceleration responses, it fails to capture the magnitude of the second peak in pitch rate, the magnitude of the following response for about 0.75 second, and the corresponding features in the normal acceleration response. The frequency content of the input shown in Fig 17c is well within the upper limit of the modelling frequency range, and although the magnitude of the input and the resulting response is large enough to suggest non-linearity through amplitude-dependent effects, the results shown in Fig 17a have similar input and response magnitudes, and the model in this case accurately predicts the helicopter's behaviour over the entire time interval. The input shown in Fig 17c does however, have a very high rate of application, and it is quite likely that actuator rate limits are being met, rather than the response characteristics to longitudinal cyclic pitch inputs themselves becoming nonlinear.

Fig 18 compares the equivalent model parameters for the augmented and unaugmented configurations, which shows that the dominant effect of the augmentation system is on the equivalent damping ratio and natural frequency. Note also from this figure that the augmentation system has the effect of slightly increasing the two equivalent delays. The equivalent delay in pitch rate is on average a very substantial 200 ms for all configurations. The Puma's actuation system has been identified elsewhere[8] as

$$\theta_{1s} = 0.00454e^{-0.106s}\eta_{1s} \tag{15}$$

indicating that half the equivalent delay in pitch rate is due to the actuation system, and half due to rotor dynamics. That this latter contribution is substantial is due in no small part to the fact that the Puma's normal rotor operating speed is a relatively slow 265 rev/min. The nature of the pitch rate delay to cyclic inputs is fully investigated in Ref 5, where it is shown that in addition, centre-of-mass location, relative to the line of action of the rotor Z-force, can significantly alter this delay term. This is because increasingly forward centre-of-mass tends to make the pitch rate response to cyclic inputs increasingly non-minimum phase in nature.

To complete this section of the Paper, Figs 19 and 20 summarise comparable modelling results for the Lynx helicopter, to those given previously for the Puma. Fig 19 shows the frequency sweep input in longitudinal cyclic, and the corresponding response in pitch rate and normal acceleration (there is no provision for incidence measurement on the Lynx as yet, and it has to be derived using rate and accelerometer data). Fig 20 shows that the Lynx pitch rate response to cyclic, like the Puma, exhibits 'classical' short-period motion form (since this helicopter's response characteristics can be captured by the model structure shown in equation (13)). The coherency function indicates that the Lynx pitch rate response to cyclic is essentially linear over most of the frequency range shown, certainly down to about 0.02 Hz (0.125 rad/s). However like the Puma, this response can only be characterised as being of 'classical' short-period form down to 0.1 Hz (0.628 rad/s), as can be seen by the growing mismatch with the equivalent system below this frequency. Comparison of the frequency response shown in Fig 20 with that shown in Fig 14b highlights difference between hingeless and articulated rotorcraft pitch response characteristics.

5 COMPARISON OF THEORY WITH EXPERIMENT

The preceding two sections have demonstrated that both high order descriptions of conventional rotorcraft, and actual flight behaviour can be represented in the conventional classical short-period form, with added time delays to accommodate high frequency phase effects. Verification of the theoretical model is addressed in this Paper by comparing the respective models' equivalent parameter sets

$$[\delta_w \ \delta_q \ \zeta \ \omega_n \ \tau_w \ \tau_q \ Z_{\theta_{1s}} \ M_{\theta_{1s}}] \ ,$$

as shown in Fig 21 for pitch models of the Puma. It is felt that such comparison gives more of a physical insight and allows easier interpretation of theoretical model inadequacies than comparison of time or frequency response. Table 3 shows a typical comparison of theory (an early version of HELISTAB) with experiment, for the Puma unaugmented at 80 kn. This shows an M_α (or M_w) deficiency in the theoretical model, if the parameters $\{\zeta \ \omega_n\}$ are considered. While the theoretical model would appear to underestimate ζ and overestimate ω_n, note that it accurately predicts equivalent total damping, given by the product of these two parameters. Therefore the equivalent stability derivatives Z_w and M_q are quite likely to be accurately captured since

$$2\zeta\omega_n = -Z_w - M_q \ . \tag{16}$$

Given that this is indeed the case, the inadequacy in ω_n, which is related to the equivalent derivatives by

$$\omega_n^2 = M_w Z_q - Z_w M_q \tag{17}$$

is due to an M_w-type or Z_q-type deficiency. Now Z_q-type effects are dominated by the speed V_f, but the earlier version of HELISTAB lacks a main rotor wake-horizontal tailplane impingement model, an aerodynamic interference effect known to make M_w more positive. Such an effect improves the inadequacy shown in Table 3. The comparisons given in Fig 21 are for equivalent systems of 12 DOF models that have been modified to incorporate a model of main rotor wake-horizontal tailplane interference. It can now be seen that apart from the equivalent parameters δ_w and $Z_{\theta_{1s}}$, which show considerable disagreement, the theoretical model is a fairly accurate representation of the Puma's behaviour measured in flight. The theoretical model's inadequacy in δ_w and $Z_{\theta_{1s}}$ is as yet unresolved, although the fact that the theoretical values appear to be simply shifted relative to the experimental results could indicate that this may have a relatively straightforward explanation. The theoretical model also fails to predict the trend in ζ and ω_n with increasing speed, particularly above 100 kn, but is accurately predicts equivalent pitching moment per unit control, the pitch rate zero and the effective pitch rate time delay throughout the speed range shown.

Fig 22 compares theoretically and experimentally derived normal acceleration parameters a_n, b_n Z_n, and it can be seen that they are accurately predicted by the theoretical model. The equivalent term Z_n is important from the model verification standpoint, particularly in relation to the $Z_{\theta_{1s}}$ result shown in the preceding figure. This is because if the normal acceleration model accurately captures the response to step inputs (as they are shown to do in Fig 17) then Z_n is a very good estimate of the actual (not equivalent) $Z_{\theta_{1s}}$ found in the full vehicle equations of motion. The evidence in Fig 22 is that the theoretical model provides a very good estimate of the real $Z_{\theta_{1s}}$.

6 FURTHER ASPECTS OF VEHICLE MODELLING

Although up till this point in the Paper the emphasis has been on the production of aircraft models that can be used to predict aircraft behaviour - what can be called quantitative modelling - the input-output coherency functions do however, add to the picture of aircraft behaviour characteristics, and in a qualitative sense complete the picture of aircraft behaviour given by the parameterised (or quantitative) models. Fig 23 for example shows the incidence and pitch rate to cyclic coherency functions for both augmented and unaugmented Puma configurations at 80 kn. Between 0.15 and 0.50 Hz (1.0 to 3.0 rad/s), the coherencies for the unaugmented configuration are higher (in fact very close to 1) than for the augmented configuration, which display a distinctive 'step down' below 0.5 Hz (3.0 rad/s). This dip in coherency is due to nonlinear augmentation system behaviour. The attitude loop in the augmentation system is disconnected when force sensing links detect that the stick is being moved from trim. This trim range is fairly wide so that for the low frequency part of the frequency sweeps, the attitude signal is reconnected for relatively long periods of time as the cyclic stick is moved forward and back through trim. The coherency functions quantify the extent to which this behaviour is nonlinear (by the magnitude at particular frequencies), and the frequency range across which it manifests itself as a noticeable nonlinearity.

The Lynx flight control system also exhibits nonlinear behaviour that has similar effects on the modelling (observable through the coherency function) as those for the Puma, although the nature of the nonlinearities is quite different. Inspection of the pitch rate and longitudinal cyclic time histories given on Fig 19 reveals a pitch rate oscillation superimposed on the overall perturbation in pitch rate that appears uncorrelated with the input. This oscillation is a known feature of the Lynx behaviour (which does not impinge adversely on the vehicle's handling qualities) and has a period of approximately 1.75 s (0.6 Hz, 3.6 rad/s); a dip in the pitch rate to cyclic coherency function can be observed on Fig 20 around this frequency. This dip is about 0.15 Hz (1 rad/s) wide, but in magnitude is relatively small, indicating that this aspect of Lynx behaviour has a small impact on the overall modelling of the short-period pitch axis dynamics.

Finally the CAC behaviour has a limiting impact on the synthesis of normal acceleration to cyclic models, as can be seen from the coherency function, Fig 24. While the model is acceptably linear up to 0.5 Hz (3 rad/s), above this it can be seen that the coherency function questions the linearity of any derived normal acceleration to cyclic frequency response. Indeed the frequency response itself has a similar appearance to the coherency function above 0.5 Hz (3 rad/s).

7 HANDLING QUALITIES

Helicopters, in common with all other aircraft, can suffer from a plethora of handling difficulties, that can manifest themselves in many ways and have root causes that are subtle in nature. It is because of this that a comprehensive specification that can be used for design, compliance demonstration and prediction (such as that proposed in Ref 1) needs to have individual criteria that address particular aspects of handling qualities. In this Paper the bandwidth criteria proposed for establishing handling qualities pertaining to tasks that require small amplitude attitude changes, is examined. The proposed criteria, as shown in initial (delay-bandwidth) and revised (phase slope-bandwidth) form in Fig 1, is designed to protect against PIO, and assure Level 1 (satisfactory) handling qualities (if complied with) in aggressive high-gain compensatory attitude tracking tasks. This section of the Paper addresses the appropriateness and correctness of these proposed criteria. The experimentally-derived models of the Puma and Lynx have been used to characterise each aircraft in terms of the proposed criteria.

7.1 Flight-testing for handling qualities

The requirements of any flight-test technique for handling qualities include repeatability consistency and relevancy - relevant both to the nature of helicopter operation, and the criteria under investigation. Consistency and repeatability is required to ensure that different pilots are performing nominally the same experiment. Relevancy to the nature of helicopter operation points towards the use of role-related experiments, ie tasks that can and do form elements of a typical mission. Relevancy to the criteria requires that the helicopter be flown in such a way

that the handling deficiencies which the given criteria are designed to highlight, do in fact manifest themselves. Evaluation of a one-on-one, air-to-air pitch tracking task in the vertical plane only, as a role-related task, proved difficult to the point of being unworkable. This task was more akin to a pursuit, rather than compensatory type, with very large speed and attitude perturbations, and proved to be neither repeatable, consistent, nor did it highlight the deficiencies that bandwidth criteria is designed to do. The task ultimately developed was a stylised pitch tracking task, where the pilots were required to track (using the attitude indicator) attitude cues called by the flight-test observer, Table 4. These cues have been designed so that their mean is approximately zero, and that the aircraft does not stray too far from the trim condition, with commanded attitude excursions limited to ±7.5°. The cues are not strictly random in nature, having been selected at 3 second intervals from a time history constructed from a sum of five equi-amplitude sine waves of varying frequency. The task is flexible, clinical and repeatable, and the cues can be designed to produce piloting control strategy that exposes latent pilot-induced-oscillation (PIO) tendencies. The resulting data is of a type amenable to analysis by spectral techniques (like the frequency sweeps) and the length of each run (typically up to 2 minutes) ensures that deficiencies and their nature are brought into focus for the test pilot. Heffley[13] has reported use of a similar task in simulator studies of roll control, the task in this case implemented by means of roll cues presented on a head-up display.

7.2 Handling qualities results

Four test pilots took part in the handling qualities evaluations, their backgrounds varying between assault, support and utility/anti-tank flying, and experience on the Puma varying from 6 to 200 hours. The formal evaluations have all been carried out using the Puma - Lynx characterisations are included for comparison only.

Fig 25 shows longitudinal control input, pitch rate, pitch attitude and air-speed perturbations from one run flown by one of the pilots at 80 kn with the augmentation system engaged. Note that for a task that requires peak attitude perturbations of ±7.5°, the rates and attitudes achieved are as high as 20°/second and 10° respectively, testifying to the task aggressiveness and to some extent the inherent vehicle deficiencies in relation to this task. The Puma of course as a support helicopter, was not designed for such usage operationally, and accordingly any deficiencies in relation to the pitch tracking task are not appropriate to the operationally flown aircraft. The attitude time history in particular clearly shows the overshoot characteristics perceived by the pilots as giving rise to a perceived degradation in task performance. This was caused by apparent overcontrol as a consequence of the large equivalent time delay in pitch. Control input autospectra for all four pilots is given in Fig 26, where it can be seen that the task is repeatable and consistent (from the point of view of applied control strategy), and that the pilot is exercising control aggressively enough to required inputs at a fairly high frequency, which is necessary for exposing latent PIO tendencies. Fig 27 shows the Puma characterisation in terms of bandwidth criteria proposed in Ref 1, and the version proposed in Ref 2 to supercede it. For the reader unfamiliar with Refs 1 and 2, it is pertinent at this stage to explain what bandwidth is, and how it is calculated. The aircraft bandwidth is that frequency which is some specified stability margin away from the attitude-to-controller phase response crossover frequency. Closed-loop control by the pilot at frequencies above the bandwidth frequency will start to degrade handling qualities as the pilot moves into the region of PIO; increasing pilot gain will degrade closed-loop tracking performance until the closed-loop pilot-vehicle system goes unstable. The stability margins specified in Refs 1 and 2 are 45° in phase or 6 dB in gain. There is evidence to suggest[14] that for the experiments conducted as part of the studies described in this Paper, the pilots operated to phase as opposed to gain stability margins; accordingly gain-limited bandwidth will not be considered further. Pilot ratings of handling qualities were returned using the Cooper-Harper[15] scale, and the averaged over the four pilots is shown next to each configuration's location in Fig 27. Average pilot ratings and corresponding standard deviation bounds are used simply because in this case they are convenient statistical measures of the collective assessments of the individual pilots. Note that two configurations are absent from these diagrams; they are unaugmented configurations whose projected bandwidth is at such a low frequency that they cannot be assessed because of a lack of confidence (as indicated by the respective coherency functions) in the modelling in this region. It can be seen that the pilot ratings do in fact display only limited correlation with the handling qualities predicted by these diagrams. For example, the unaugmented configurations are not rated nearly so badly by the pilots, and the augmented configurations are assessed firmly as Level 2 (acceptable), although on the diagrams they appear marginal Level 1 to 2. Note the improvement in the handling qualities ratings given by the pilots when the aircraft centre-of-mass is moved forwards, and the equivalent time delay is reduced by around 50 ms. The relatively large equivalent delay of around 200 ms has been commented on by all participating aircrew repeatedly as being intrusive and contributing significantly to the degradation in the augmented configuration's rating from Level 1 to Level 2. To explore the inadequacies and appropriateness of the proposed criteria, Fig 28 shows the variation in pilot rating with bandwidth and phase slope. Note firstly that there is a fairly broad range of bandwidths (about 1 rad/s) over which the pilot rating does not change. These locations lie in that area of the criteria diagrams where such a variation in bandwidth is predicted to vary the handling qualities from Level 1 to Level 2. Secondly, note that over a substantial range in values of phase slope, the handling qualities also appear not to vary. For the relevant configurations, the equivalent delays also vary by an insignificant amount (the equivalent delays are annotated to the relevant test points on Fig 28a), and so the 'flat spot' in vehicle rating with bandwidth cannot be explained by improvements in phase slope or delay: similarly the apparent insensitivity of pilot rating with phase slope cannot be explained by the required variation in bandwidth.

Examples of the identification of pilot control strategy used to resolve the inconsistencies outlined above, are shown in Fig 29. Comparisons between the pitch rate to longitudinal cyclic models of the Puma identified from the frequency sweep (open-loop) data, with those obtained from the tracking (closed-loop) experiment, are for the 80 kn augmentation engaged configuration. It is clear across which frequency, range, and up to which frequency, the pilots are required to apply compensation as a consequence of the task demands. This 'peak pilot operating frequency' has been obtained for each pilot-vehicle combination, and used to calculate the

effective phase margins to which each pilot operates. The two configurations with varied centre-of-mass location are excluded from this analysis, since their rating is directly influenced by the variation in the effective delay, and its perceived effect on handling qualities. For all the other configurations, the averaged pilot ratings with standard deviation bounds, are plotted against the averaged effective phase margins, Fig 30. There is, as to be expected given the philosophy behind the use of bandwidth as a handling qualities parameter, a quite obvious relationship between pilot rating and the proximity to the phase crossover frequency that the pilot is required to operate by the task demands (which is what the effective phase margin is). The form of this relationship too, is as might be expected, that of pilot rating being degraded progressively only below a particular phase margin. Fig 30 does however, suggest that this phase margin is in fact about 30° and not 45°, which is the value given in Refs 1 and 2. Note that the curve drawn through the points on Fig 30 is asymptotic to a pilot rating value of about 4 (ie Level 2), indicating that there is some effect other than bandwidth degrading the handling qualities. It was indicated previously that pilot rating does not seem to be affected by phase slope, but that the pilots repeatedly highlighted what they felt to be excessive effective delay in pitch. Two pilots flew the aft centre-of-mass configuration immediately after flying the forwards loaded configuration, and commented that the effective time delay appeared much less intrusive, and accordingly rated the aircraft one pilot rating better, ie now in Level 1. The difference in effective delay between these two configurations is around 50 ms, and it is tentatively suggested therefore that a decrease in pitch axis delay of this amount is sufficient to improve the pilot ratings by one point. This correlates with fixed-wing experience and the apparent level of the asymptote in Fig 30. Combined with the qualitative pilot comments for these configurations (which emphasised the intrusiveness of the effective delay), the evidence is that the asymptote on Fig 30 lies at a value of 4 because of delay effects.

The results tend to indicate that for the Puma flying the task described, phase slope-bandwidth criteria is neither appropriate nor correct for establishing handling qualities in small perturbation compensatory tracking tasks. Objective and subjective (pilot-based) analysis indicates however, that equivalent (phase) delay-bandwidth criteria is appropriate, with the incorrectness being resolved in a rational fashion and on a consistent basis. This can clearly be seen from a perusal of Fig 31, which shows the delay-bandwidth diagram redrawn to incorporate the results of the analysis outlined above. The Level 1 to 2 boundary has been redrawn to limit Level 1 handling qualities to configurations with effective delays less than at least 200 ms, and with a stability margin of 30° in phase used to establish bandwidth. Use of this margin has the effect of moving all the points on Fig 27 to the right, to their new locations as shown on Fig 31. For the unaugmented configurations, this places all four on the diagram such that there is now good correlation between the handling qualities predicted by the criteria given on Fig 31, and the actual ratings returned by the pilots. For the augmented configurations, they all now lie in a region of the diagram where the boundaries are such that a variation in bandwidth of 1 rad/s does not imply a variation in handling qualities of between Level 1 and Level 2.

The Lynx is shown on this diagram to be firmly in the Level 1 zone. Although a full programme of handling qualities assessment of this aircraft has only recently got underway, initial tentative impressions of the Lynx are that for the task described in this Paper, the aircraft does indeed have Level 1 handling qualities. The aircraft response displays no overshoot when flown aggressively in the tracking task, and it does not display incipient PIO tendencies. Effective delay is still noticeable, but not intrusive to the extent that it can degrade handling qualities from Level 1 to Level 2.

8 DISCUSSION

The developing handling qualities specifications are requiring accurate descriptions of rotorcraft behaviour, because of their comprehensiveness and the specific and detailed nature of the individual criteria that make up these specifications. It is for this reason that system identification needs to become an integral element of the handling qualities engineer's toolkit. This is to provide vehicle models in circumstances where theoretical models have known deficiencies, and also to allow upgrading of such models to the extent that they can be used with confidence at the design stage and in compliance demonstration, thus saving on expensive and time-consuming flight-testing. Model reduction to lower order forms also has an important role to play in system identification, in the analysis of handling qualities and in understanding complex vehicle behaviour. The results in this Paper have emphasised the applicability of the equivalent systems approach to problems in helicopter mathematical modelling. Insight into the flight behaviour characterised by high order descriptions of the helicopter is provided that would otherwise be impossible to achieve. An example of this is the comparison of the flight-derived equivalent system parameters with those derived theoretically, that indicated a deficiency in the static incidence stability in the 12 DOF model. Modification of this model and subsequent comparison with flight tends to verify the nature of this deficiency. This result is a simple yet practical demonstration of one of the major aims of any system identification exercise. As well as greater insight into, and understanding of inherently complex vehicle characteristics, model reduction is also important from the handling qualities perspective, since it characterises the vehicle in a form familiar to the test pilot. These model parameters relate directly to pilot-perceived aspects of helicopter behaviour such as damping, control power and natural frequency. Pilots after all do not 'see' helicopter response as a 12 DOF system, but more in the form of the model structures given in equations (13) and (14). In this Paper, the validity and robustness of these flight-derived models has been explored through verification using multi-step inputs of varying amplitude, direction of application and duration: the models have been shown to predict the helicopter's transient response to control inputs. This should be an essential step in any system identification exercise; for the cases presented in this Paper, it helps to quantify the impact of any of the nonlinearities etc, suggested by values of coherency function less than 1.

With regard to handling qualities, the results given in this Paper suggest modification of delay-bandwidth criteria in two important areas (the Level 1 to 2 boundary and the phase stability margin), and indicate that phase slope-bandwidth criteria, as currently formulated, may be both inappropriate and incorrect. These results must be kept in perspective, since they are

limited in scope to only four test pilots and one aircraft type, although this one type does offer a broad range of location on the relevant diagrams. Nonetheless the analysis that has been performed does provide a rational and consistent basis for the justification of the conclusions drawn, and in these terms the results are certainly viable and will provide a suitable basis for further exploration of bandwidth criteria, notably with the Lynx. A central concern for the future is the sensitivity of criteria to task type (or more importantly task frequency and pilot aggression), since it is known that the severity of the task and the required level of task performance can influence pilot rating. The consequence of this for criteria such as those shown in Fig 1, is that they are really only appropriate to the tasks used to develop them; accordingly, these tasks should represent a 'worst case'. Alternatively some measure of task frequency should be incorporated into the criteria, so that it becomes applicable to many different types, flying appropriate tasks. It is hoped to explore and develop these ideas in the future; the clinicality, repeatability and degree of control over pilot control strategy offered by the pitch tracking task described, makes it ideally suited for further investigation of these areas of development. The use of stylised manoeuvres in handling qualities research has been a developing area at RAE[16] for several years, and the pitch tracking task joins this suite of developing flight assessment and analysis methods.

9 CONCLUSIONS

The results demonstrate the applicability of the equivalent systems approach for characterising fundamentally complex behaviour of conventional single main and tail rotor helicopters. Model identification and reduction has indicated that the short-period pitching motion of articulated and hingeless rotor helicopters can exhibit classical form, and that higher order (rotor and actuation) dynamics contribute significantly to the overall control response characteristics as a delay effect. The Paper questions the appropriateness and correctness of two proposed handling qualities criteria based on bandwidth. It is suggested that phase slope-bandwidth criteria may be inappropriate for characterising the small amplitude tracking task handling qualities of helicopters. Evidence is given however, to show that delay-bandwidth criteria are appropriate. The observed inadequacies in this case are possibly due to the application of conservative stability margins in the calculation of bandwidth, and a Level 1 boundary that ought to restrict Level 1 handling qualities to aircraft with equivalent delays of less than 200 ms.

NOMENCLATURE

A	system matrix
B	control matrix
CAC	computer acceleration control
DOF	degree-of-freedom
F	mismatch frequency response
G_{xy}	frequency response relating input y to output x
G'_{xy}	equivalent system frequency response
$\underline{G}$	transfer function matrix
$\hat{G}_{xx}$	measured x-variable autospectrum
$\hat{G}_{yy}$	measured y-variable autospectrum
$\hat{G}_{xy}$	measured x-y cross spectrum
$\hat{H}_{xy}$	flight-derived frequency response relating input y to output x
I	identity matrix
Im	imaginary part of complex number
J	cost function
M_w , M_α etc	pitching moment derivatives with respect to vertical velocity incidence etc
PIO	pilot-induced oscillation
Re	real part of complex number
V_f	airspeed (kn)
W_g , $W_{\dot{p}}$	gain and phase weighting terms
a_n , b_n	normal acceleration transfer function numerator constants
c , d	real and imaginary parts, respectively, of $\hat{G}_{xy}$
j	number of frequency responses used in equivalencing procedure
k	number of elements in state vector
l	number of elements in control vector
m	number of points in frequency range
n	normal acceleration (g units or m/s^2)
q	pitch rate (rad/s or deg/s)
s	seconds or Laplace operator
t	time (seconds)
u	l-element control vector
w	vertical velocity (m/s)
x	k-element state vector
α	incidence (rad or deg)
γ^2_{xy}	input-output coherence
δ_α , δ_q	incidence and pitch rate transfer function equivalent zeros
θ_{1s}	longitudinal cyclic pitch (rad)
η_{1s}	longitudinal cyclic stick position (%)
τ_α , τ_q etc	incidence, pitch rate transfer function equivalent time delays, etc
θ	pitch attitude (rad or deg)

NOMENCLATURE (concluded

ζ	transfer function equivalent damping ratio
ω	frequency (rad/s or Hz)
ω_n	transfer function equivalent natural frequency (rad/s)
ϕ_p	peak pilot operating frequency effective phase margin (deg)
$\Phi_{\omega\theta}$	phase slope (s)

REFERENCES

1 R. H. Hoh et al, Proposed airworthiness design standard-handling qualities requirements for military rotorcraft, Systems Technology Inc Technical Report 1194-2 (1985)

2 R. H. Hoh et al, Proposed handling qualities specification for military rotorcraft, Volume 1 - Requirements, Systems Technology Inc Technical Report 1194-4 (1987)

3 Anon, DEF STAN 00-770, Volume 2 - Revision of Part 6 - Aerodynamics and flying qualities (rotorcraft), Joint Airworthiness Committees JAC Paper 1128, Issue 1 (1986)

4 Jane Smith, An analysis of helicopter flight mechanics Part 1 - User's guide to the software package HELISTAB, RAE Technical Memorandum FS(B) 569 (1984)

5 S. S. Houston, The effect of higher order dynamics on helicopter short-period handling parameters, RAE Technical Memorandum in preparation (1987)

6 J. S. Bendat and A. G. Piersol, Engineering applications of correlation and spectral analysis, John Wiley and Sons (1980)

7 M. B. Priestley, Spectral analysis and time series, Academic Press (1981)

8 S. S. Houston and Lt Cdr R. I. Horton RN, The synthesis of helicopter mathematical models for the prediction of control response and handling qualities, RAE Technical Memorandum in preparation (1987)

9 M. B. Tischler et al, Frequency domain identification of XV-15 tilt-rotor aircraft dynamics, AIAA-83-2695, Paper presented at AIAA/AHS/DES/SETP/SFTE/DGLR 2nd Flight Testing Conference (1983)

10 M. B. Tischler et al, Identification and verification of frequency-domain models for XV-15 tilt-rotor aircraft dynamics, Paper presented at 10th European Rotorcraft Forum (1984)

11 M. B. Tischler et al, Frequency domain identification of XV-15 tilt-rotor aircraft dynamics in hovering flight, Journal of the American Helicopter Society, 30, 2 (1985)

12 M. B. Tischler et al. Demonstration of frequency-sweep testing technique using a Bell 214-ST helicopter, NASA TM 89422 (1987)

13 R. K. Heffley et al, Study of helicopter roll control effectiveness criteria, NASA CR 177404 (1986)

14 S. S. Houston and Lt Cdr R. I. Horton RN, An examination of bandwidth criteria for helicopter pitch axis handling qualities, RAE Technical Memorandum FS(B) (1987)

15 G. E. Cooper and R. P. Harper Jnr, The use of pilot ratings in the evaluation of aircraft handling qualities, NASA TN-D-5153 (1969)

16 G. D. Padfield and M. T. Charlton, Aspects of RAE flight research into helicopter agility and pilot control strategy, Paper prepared for presentation at Handling Qualities Specification MIL Spec 8501 Update Specialists' Meeting; Aeroflightdynamics Directorate, Ames Research Center (1986)

Table 1

SUMMARY OF EXPERIMENTAL TEST POINTS

Aircraft	Flight Number	Speed (kn)	Height (ft)	Augmentation	Mass (kg)	CG
Puma	685/00/01	60	3000	No	5500	MID
Puma	685/15/01	80	3000	No	5500	MID
Puma	689/06/01	100	3000	No	5500	MID
Puma	689/11/01	120	3000	No	5500	MID
Puma	685/01/01	60	3000	Yes	5500	MID
Puma	685/10/01	80	3000	Yes	5500	MID
Puma	689/03/01	100	3000	Yes	5500	MID
Puma	689/06/01	120	3000	Yes	5500	MID
Puma	722/03/04	60	1000	Yes	5500	FWD
Puma	723/06/11	60	1000	Yes	5500	AFT
Lynx	115/01/01	60	3000	Yes + CAC	4700	MID
Lynx	115/04/01	80	3000	Yes + CAC	4700	MID
Lynx	115/08/01	100	3000	Yes + CAC	4700	MID

Table 2

COMPARISON OF NORMAL ACCELERATION MODEL TRANSFER FUNCTION PARAMETERS

Parameter	Parzen (Smooth) Window	Daniell (higher resolution) Window
a_n	0.00466	-0.07556
b_n	7.60585	7.76743
ζ	0.42849	0.44201
ω_n	1.74767	1.74174
τ_n	0.10250	0.11274
Z_n	0.00998	0.01016

Table 3

PUMA, 80 kn - COMPARISON OF THEORY WITH EXPERIMENT - PREMODIFIED HELISTAB

Parameter	Theory	Experiment
δ_w	4.67	2.12
δ_q	-1.03	-1.07
ζ	0.61	0.77
ω_n	1.45	1.13
τ_w	0.02	0.01
τ_q	0.08	0.07
$Z_{\theta_{1s}}$	-48.05	-25.90
$M_{\theta_{1s}}$	6.15	5.73

Table 4

ATTITUDE COMMAND TIME HISTORY CALLED BY FLIGHT TEST ENGINEER

Time (s)	0	3	6	9	12	15	18	21	24	27	30
Command (°)	0	-2.5	+2.5	0	-5	+2.5	-5.	-7.5	+5	0	-2.5
Time (s)	33	36	39	42	45	48	51	54	57	60	63
Command (°)	-5	0	+5	-7.5	+2.5	-2.5	+5	-7.5	-5	+2.5	-2.5
Time (s)	66	69	72	75	78	81	84	87	90	93	96
Command (°)	0	+2.5	-5	-7.5	-5	+2.5	-2.5	+2.5	+5	0	0

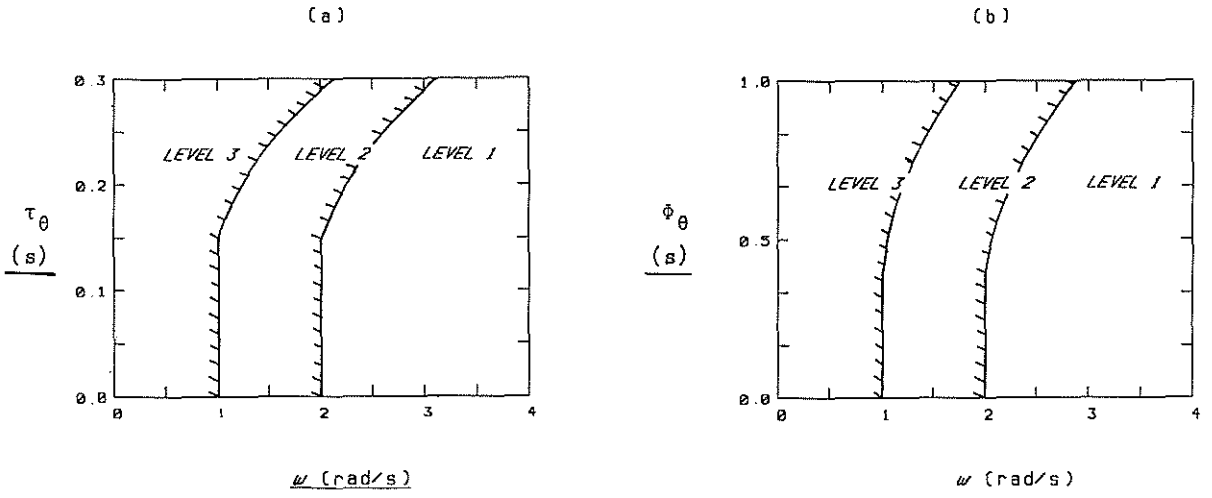

Figure 1 -- Proposed bandwidth criteria for handling qualities
(a) -- from Ref 1; (b) -- from Ref 2

Figure 2 -- RAE Bedford Puma flight research helicopter

Figure 3 -- RAE Bedford Lynx flight research helicopter

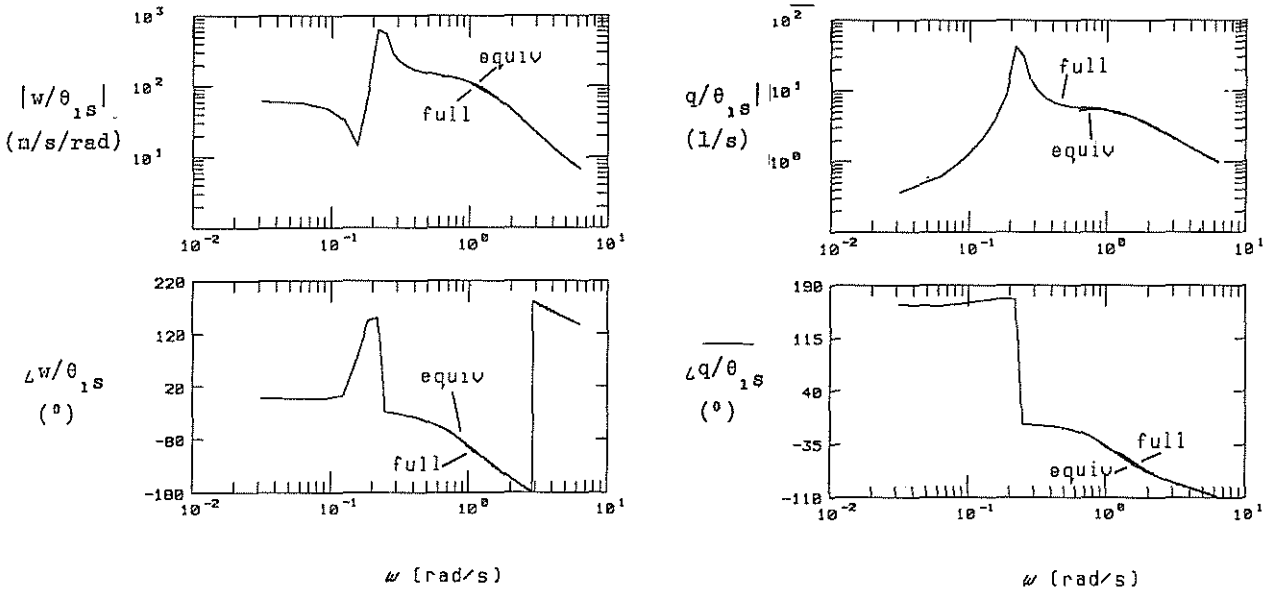

Figure 4 -- Puma, 60kn Comparison of full (12 DOF) and equivalent models

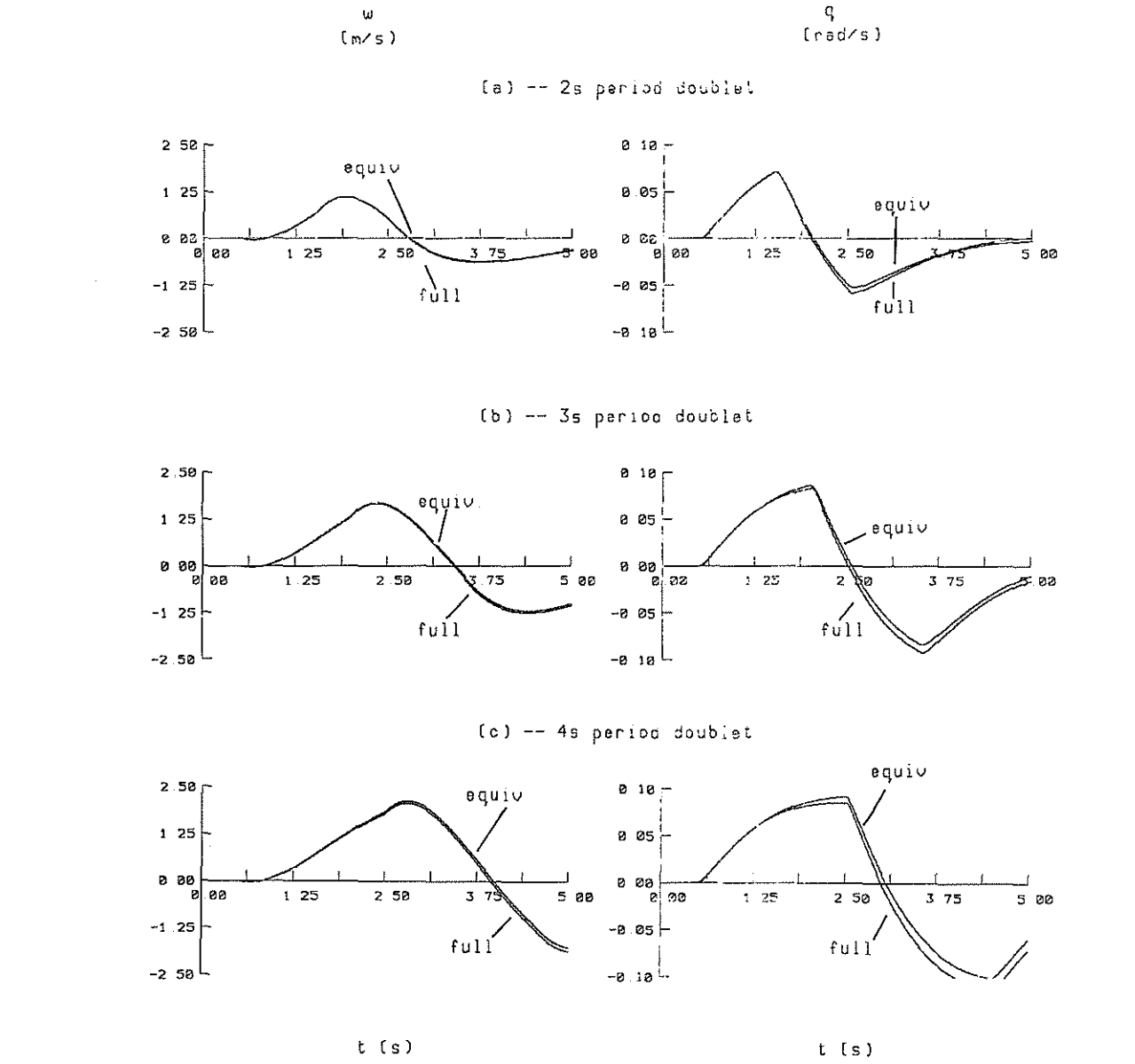

Figure 5 -- Puma, 60kn. Comparison of full (12 DOF) and equivalent models

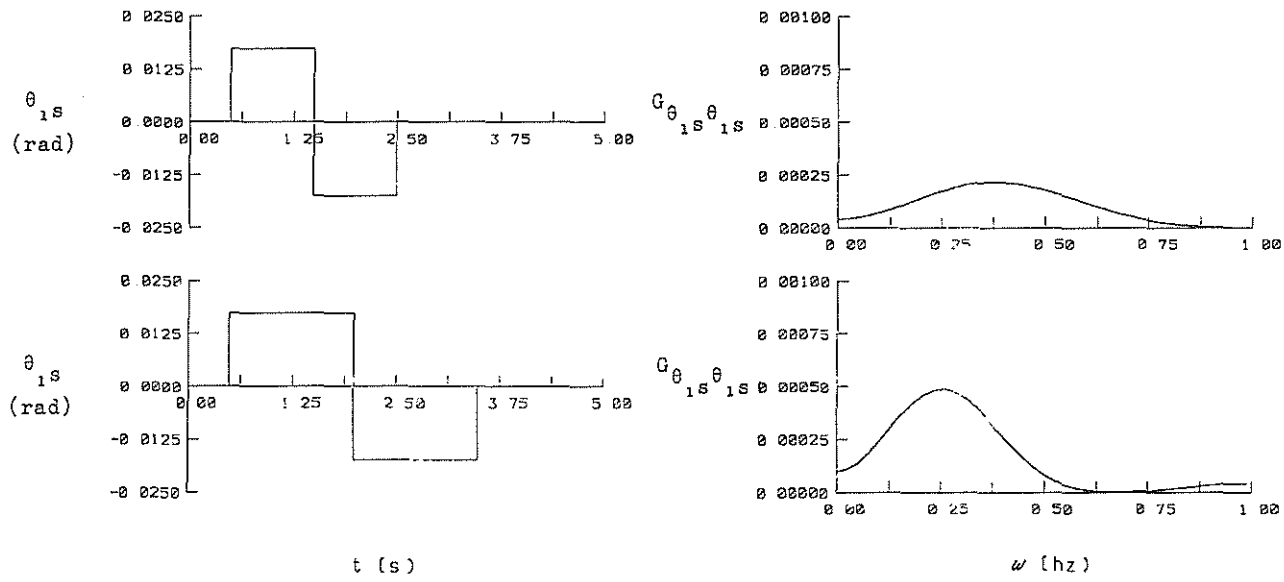

Figure 5a -- Comparison of doublet inputs and corresponding frequency content

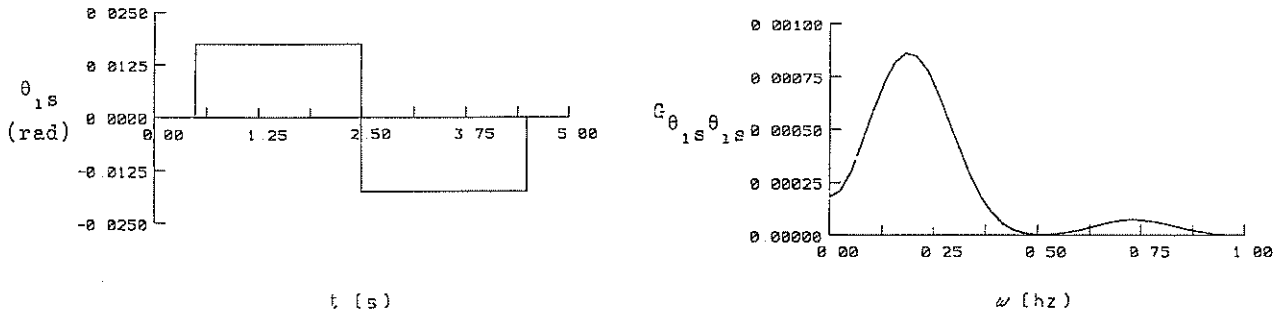

Figure 5a -- (concluded)

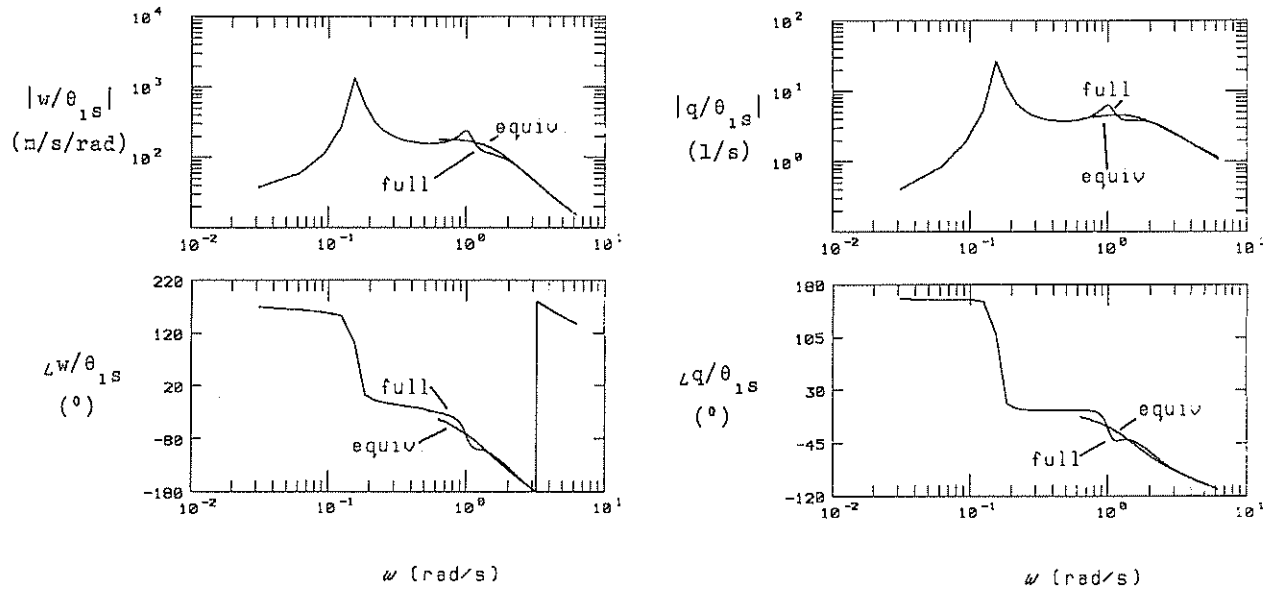

Figure 6 -- Puma, 120kn Comparison of full (12 DOF) and equivalent models.

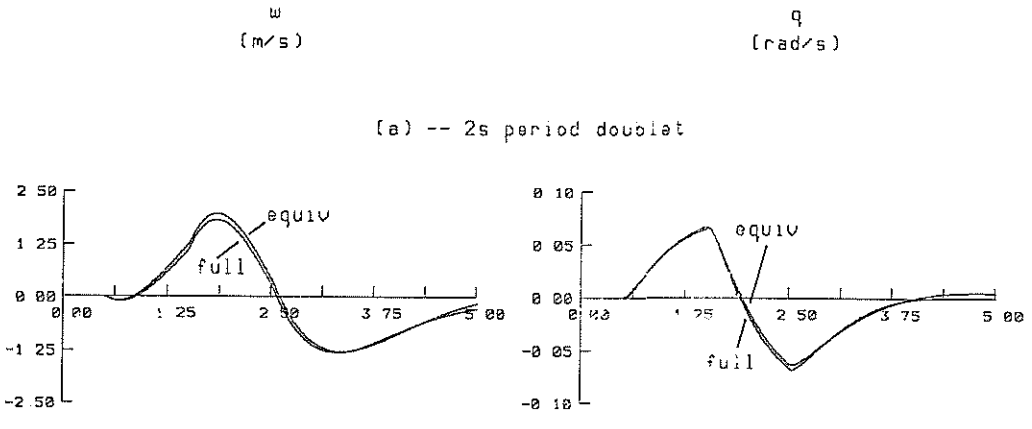

(a) -- 2s period doublet

Figure 7 -- Puma, 120kn Comparison of full (12 DOF) and equivalent models

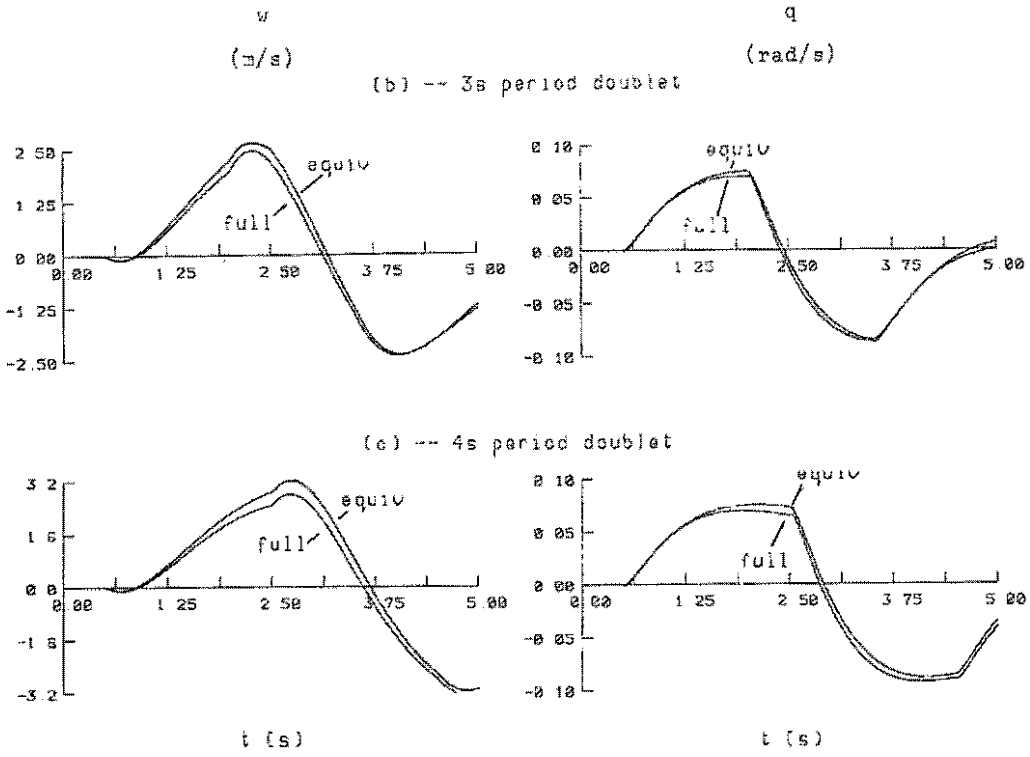

Figure 7 -- (concluded)

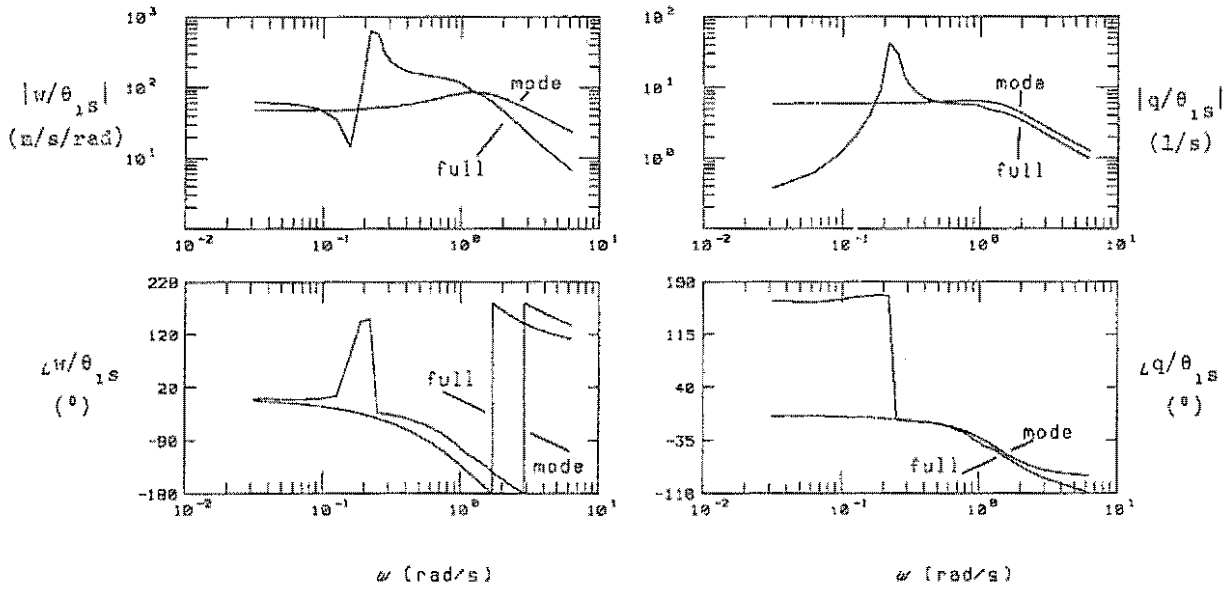

Figure 8 -- Puma, 80kn Comparison of full (12 DOF) model and short-period mode contribution

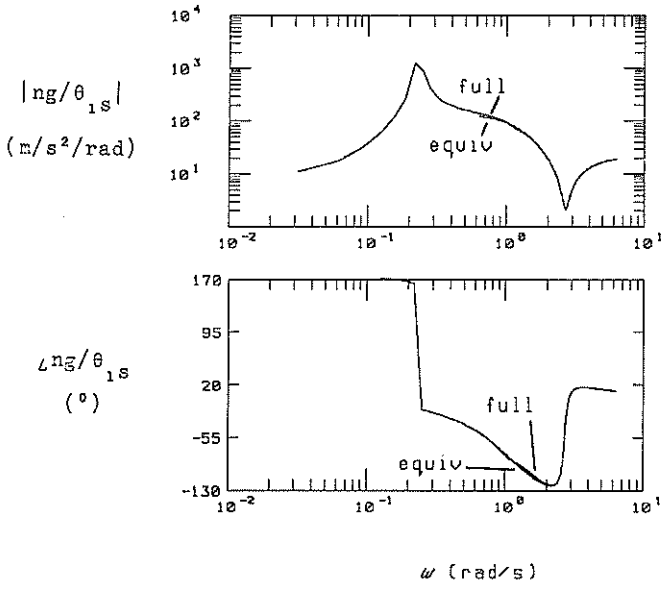

Figure 9 -- Puma, 60kn Comparison of full (12 DOF) and equivalent models.

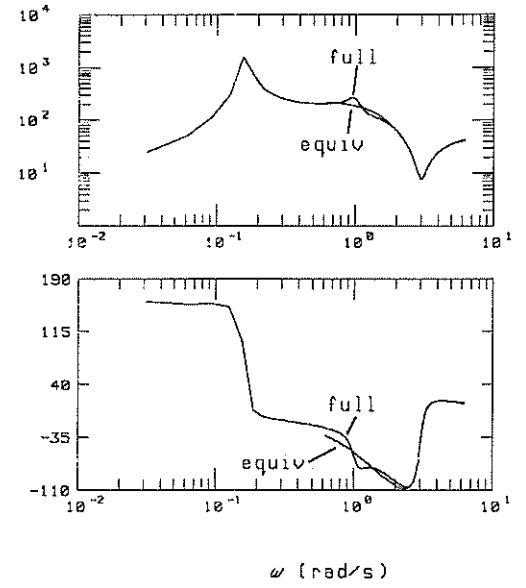

Figure 10 -- Puma, 120kn. Comparison of full (12 DOF) and equivalent models

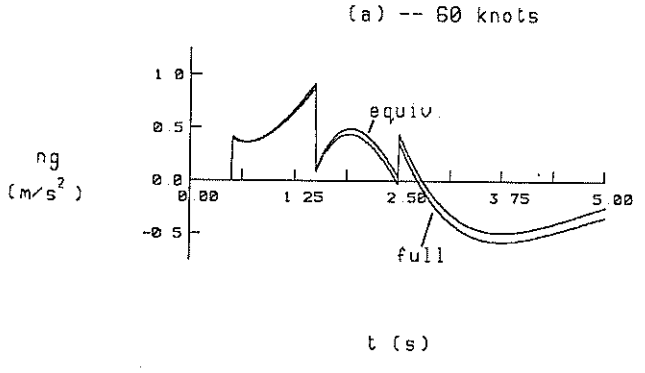

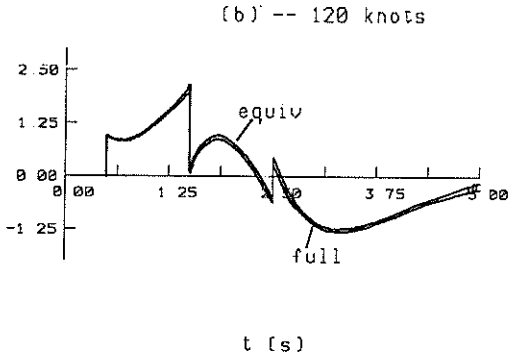

Figure 11 -- Puma Comparison of full (12 DOF) and equivalent models
(a) -- 60kn, (b) -- 120kn

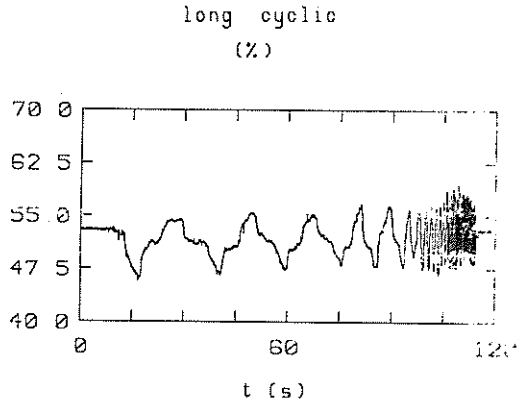

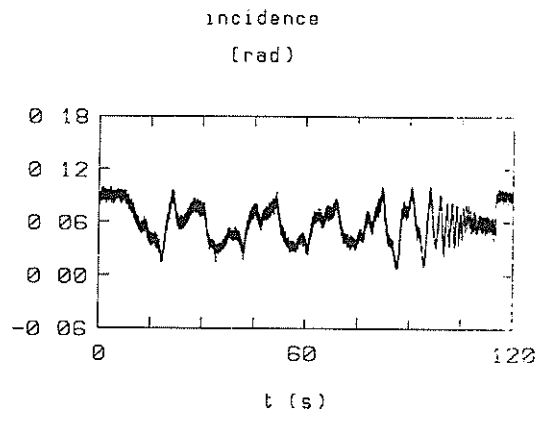

Figure 12 -- Puma XW241, flight 723/06/11 Long cyclic frequency sweep

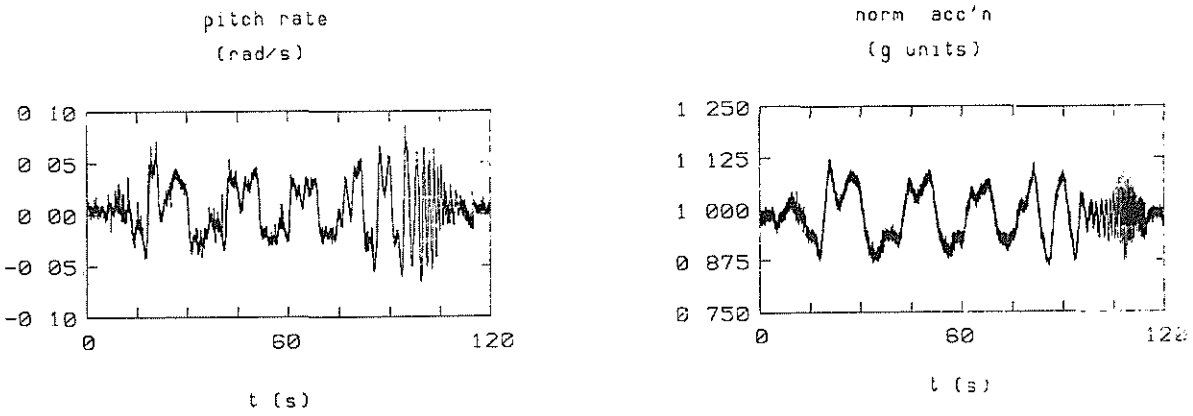

Figure 12 -- (concluded)

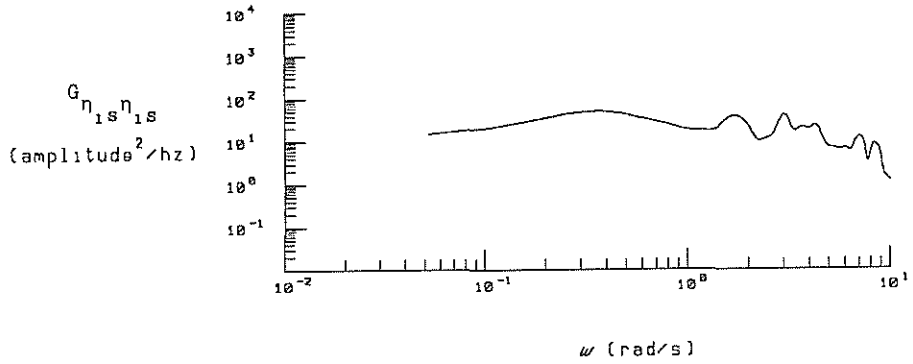

Figure 13 -- Puma XW241, flight 723/06/11 Long. cyclic frequency sweep input autospectrum

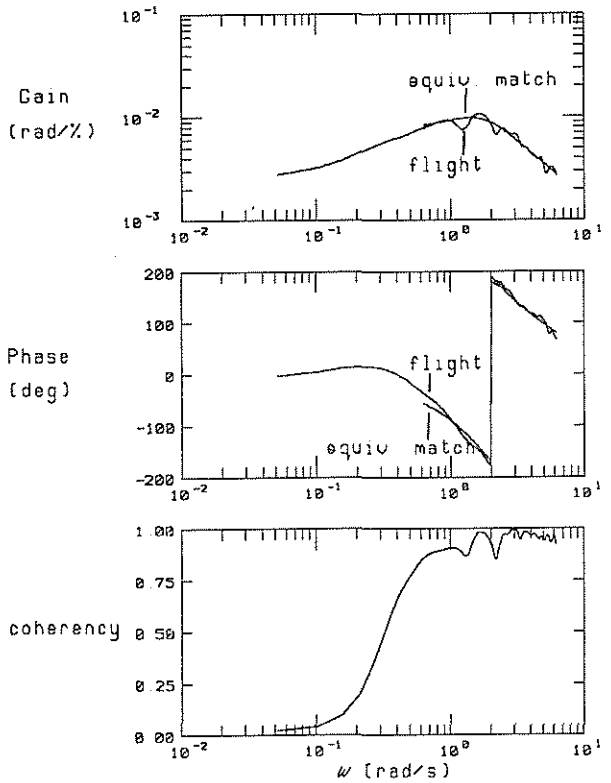

Figure 14a -- Puma XW241, flight 723/06/11 Incidence/ longitudinal cyclic modelling

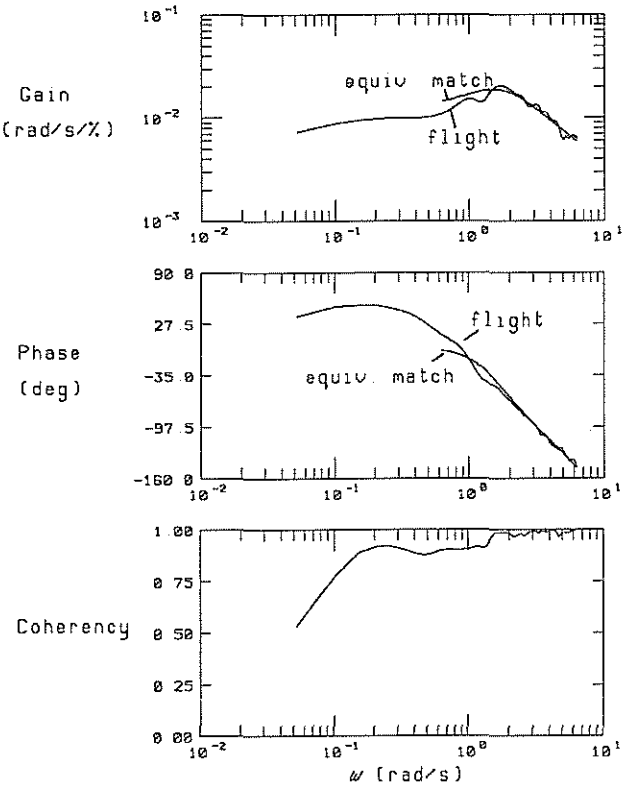

Figure 14b -- Puma Xw241, flight 723/06/11 Pitch rate longitudinal cyclic modelling

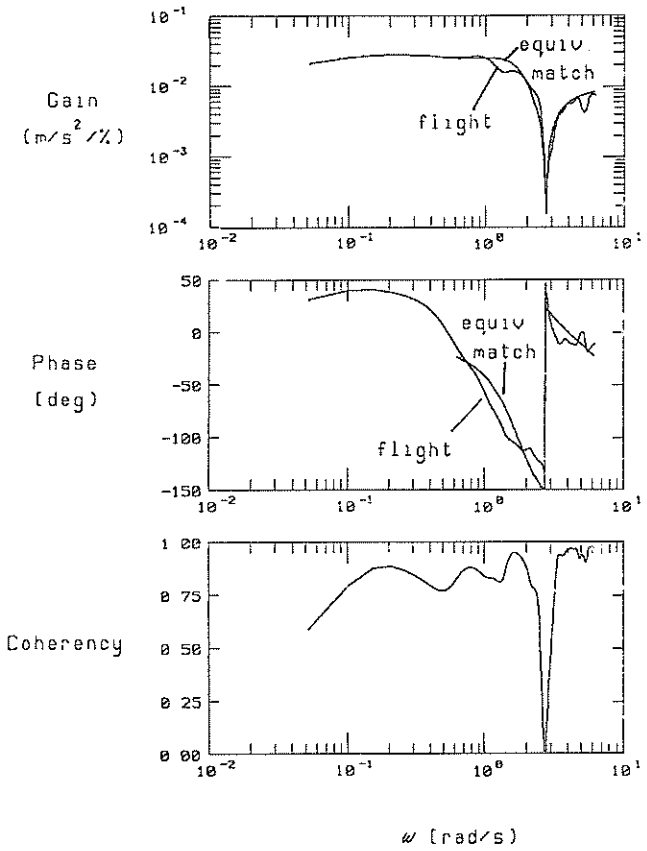

Figure 15 -- Puma XW241, flight 723/06/11 Normal acceleration/longitudinal cyclic modelling

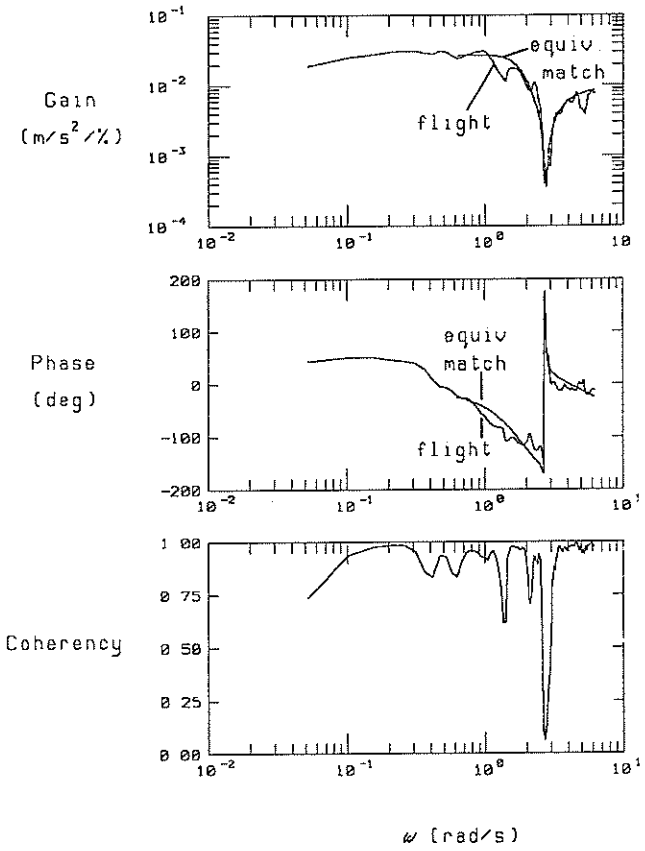

Figure 16 -- Puma XW241, flight 723/06/11 Normal acceleration/longitudinal cyclic modelling Daniell window

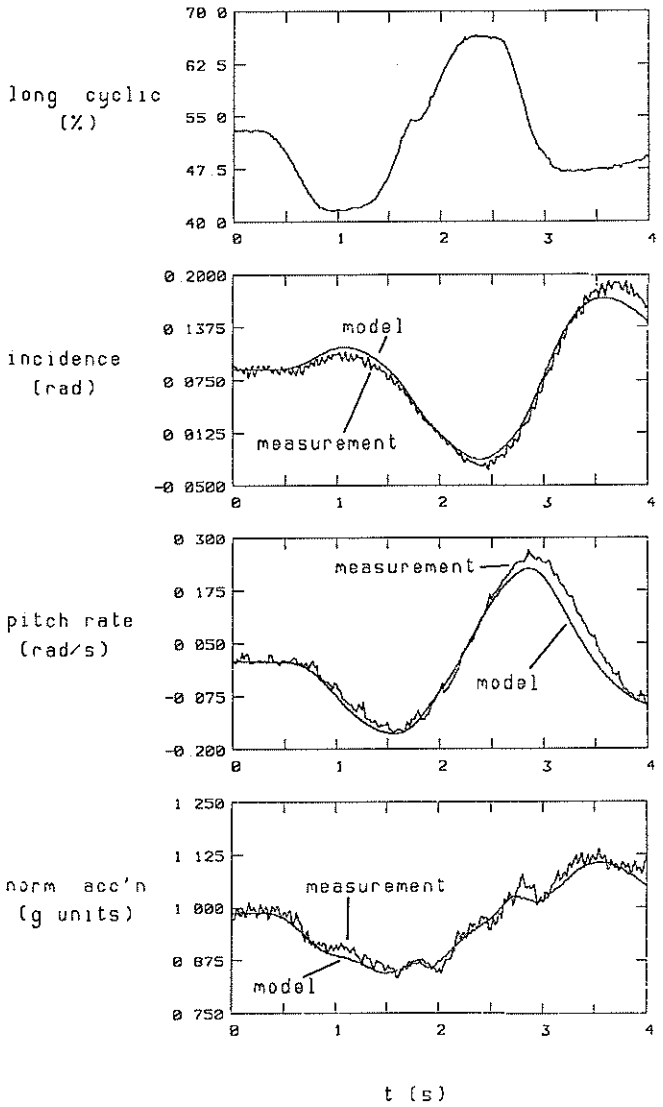

Figure 17a -- Puma XW241 Verification of model derived from flight 723/06/11

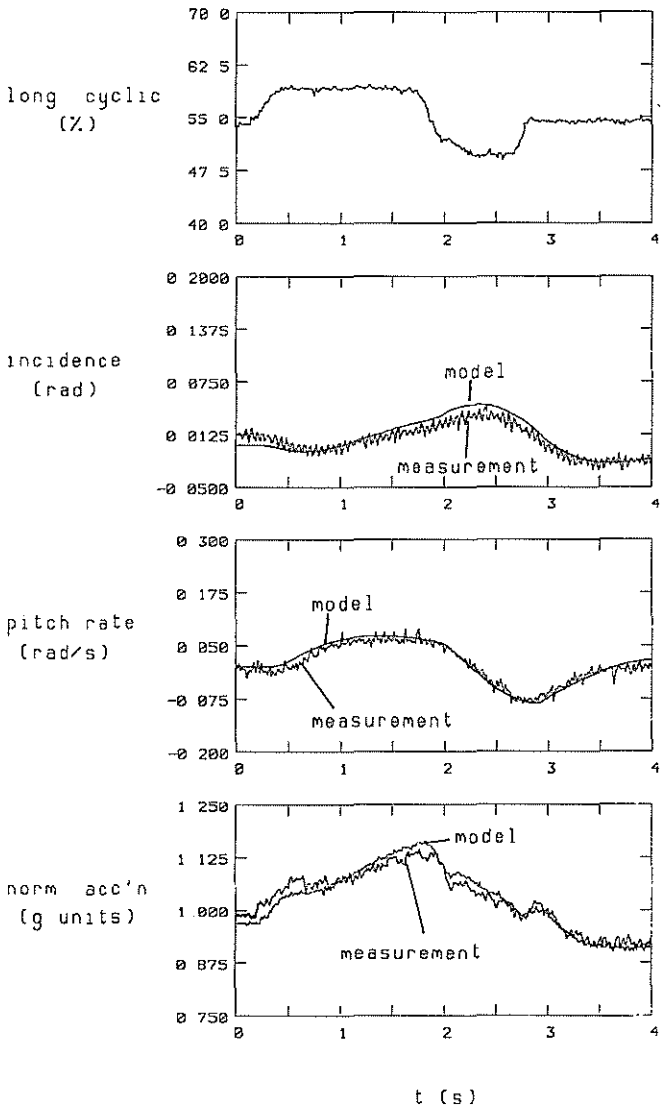

Figure 17b -- Puma XW241 Verification of model derived from flight 685/10/01

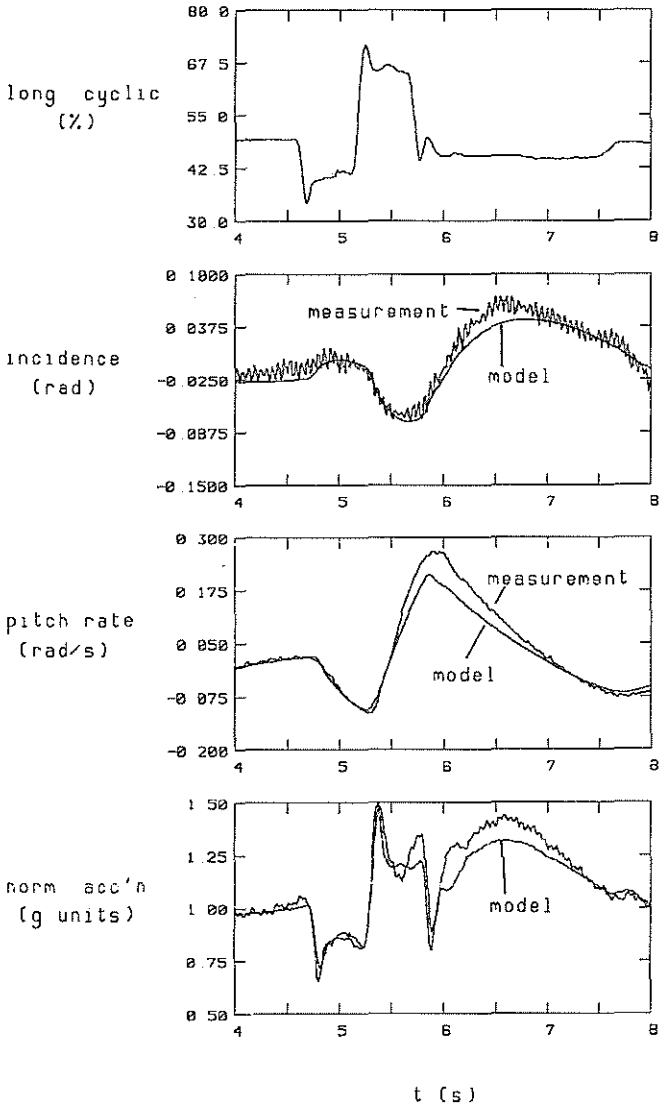

Figure 17c -- Puma XW241 Verification of model derived from flight 689/06/01

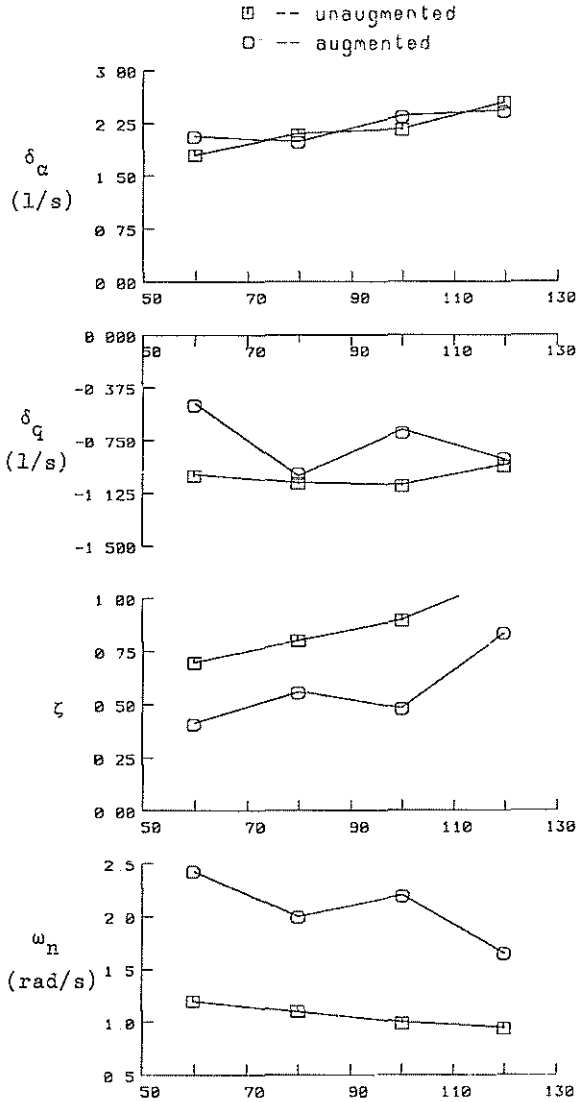

Figure 18 -- Comparison of flight-derived equivalent system parameters

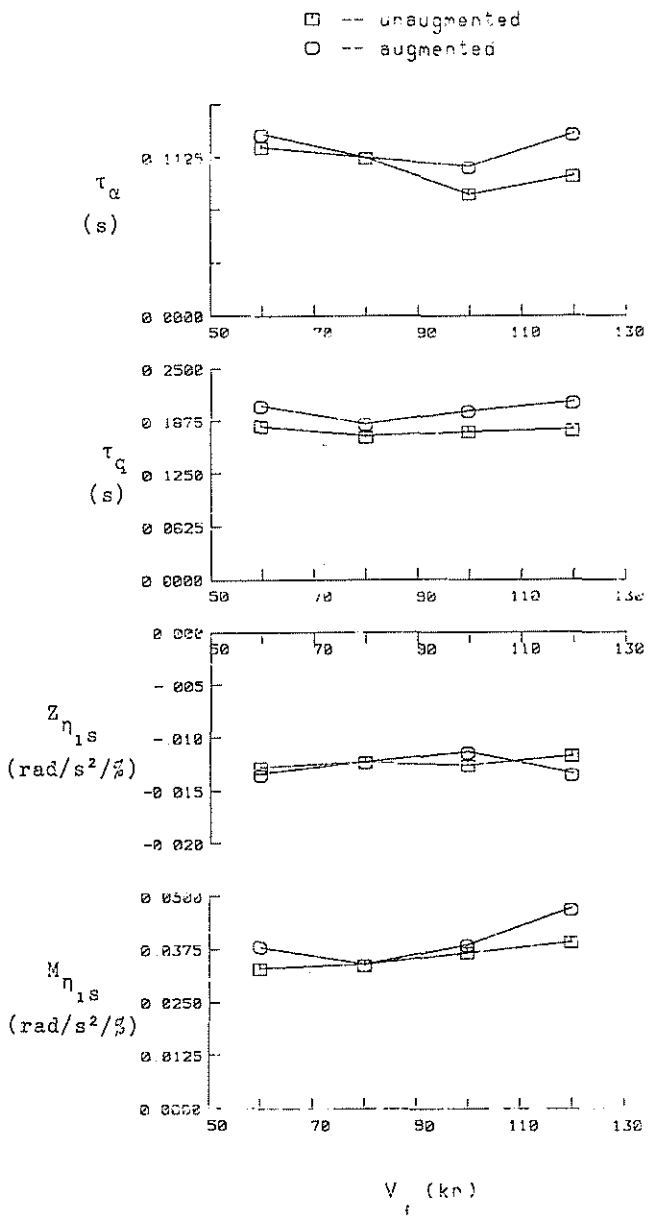

Figure 18 -- (concluded)

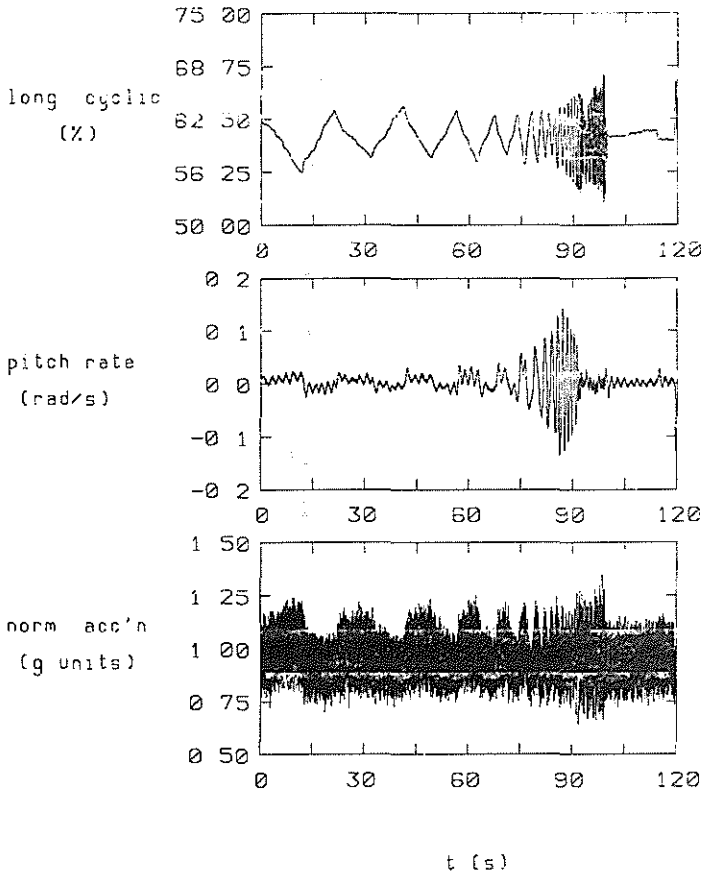

Figure 19 -- Lynx ZD559, flight 115/08/01 Longitudinal cyclic frequency sweep

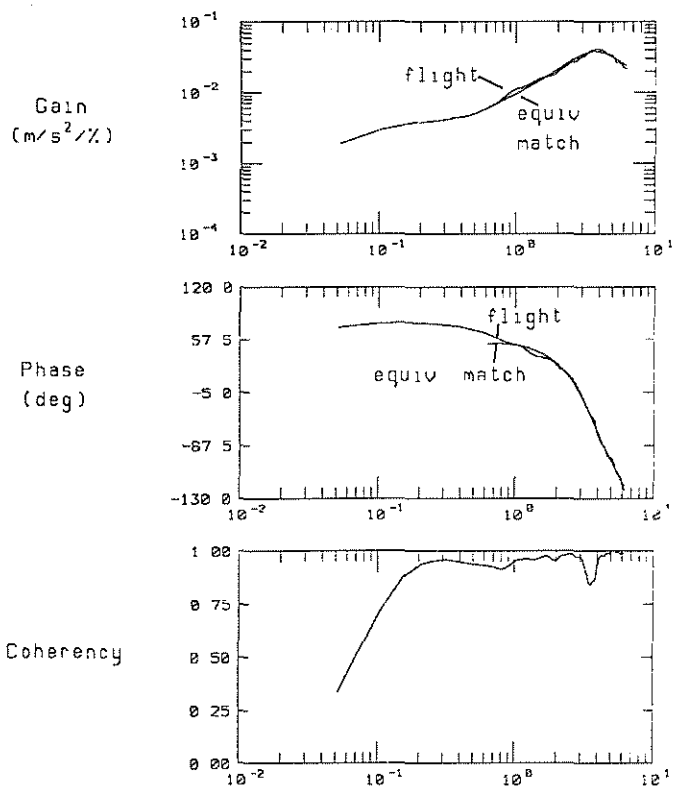

Figure 20 -- Lynx ZD559, flight 115/08/01 Pitch rate/longitudinal cyclic modelling

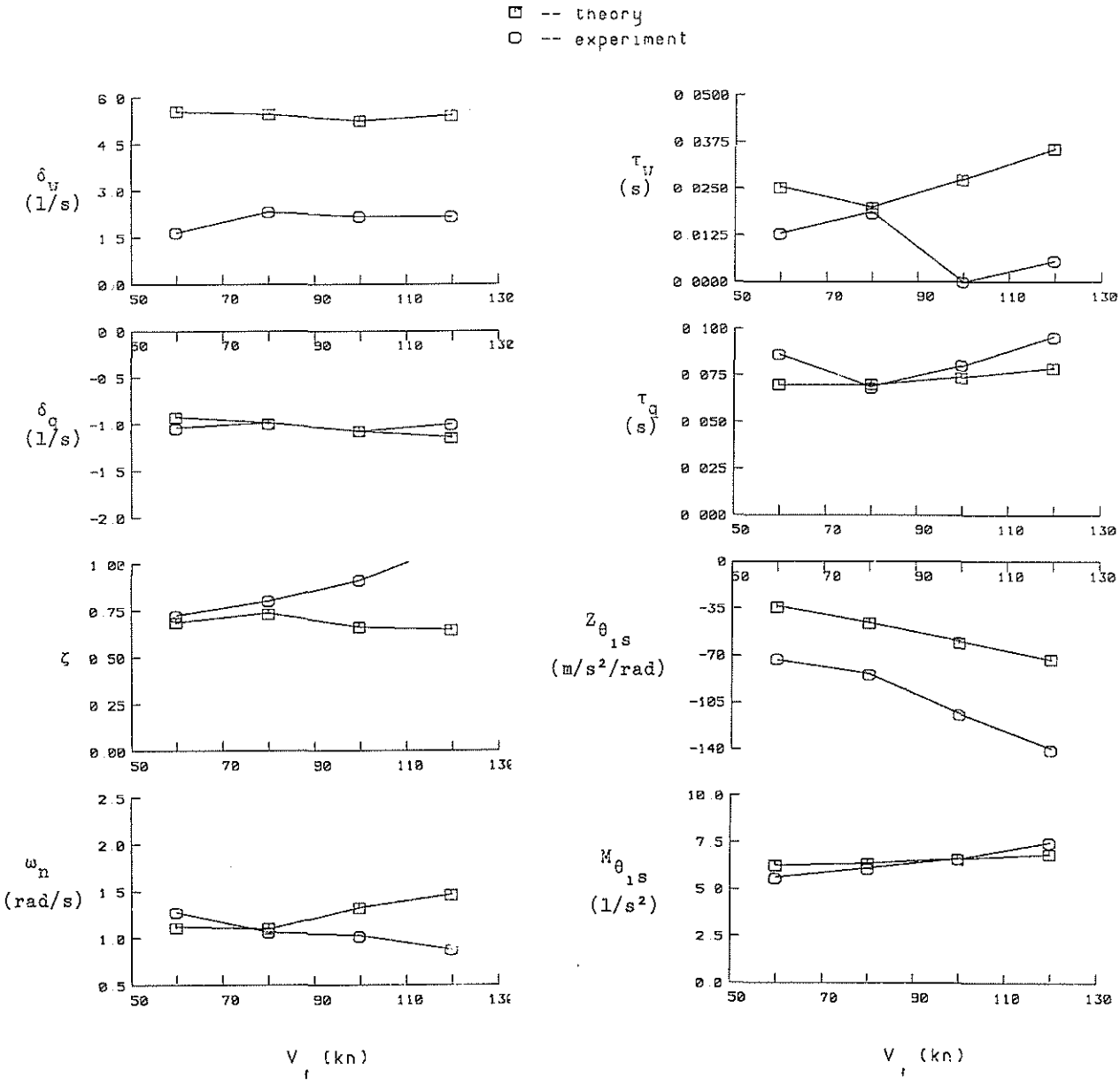

Figure 21 -- Comparison of theory with experiment HELISTAB and flight- derived equivalent system parameters

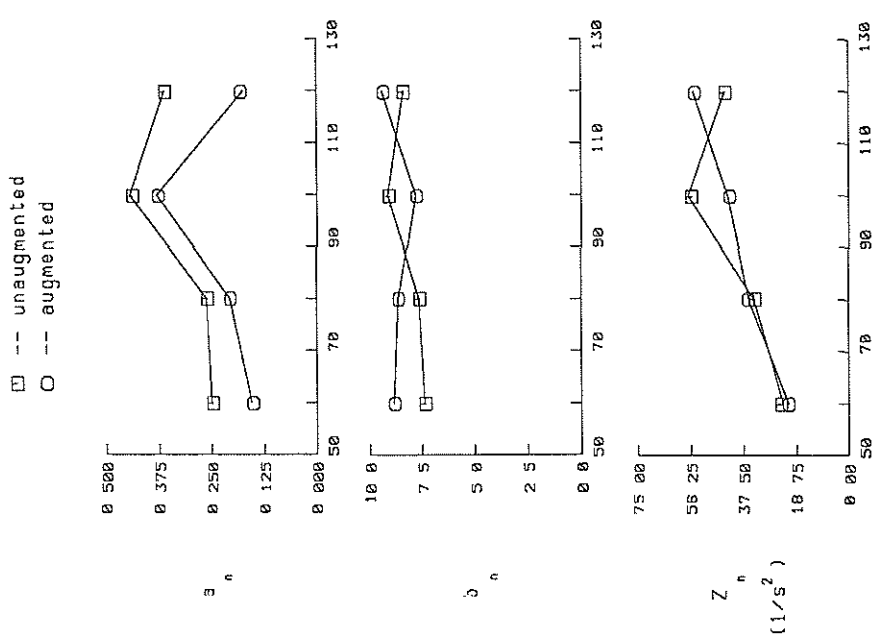

Figure 22 -- Comparison of theory with experiment HELISTAB and flight-derived equivalent system parameters

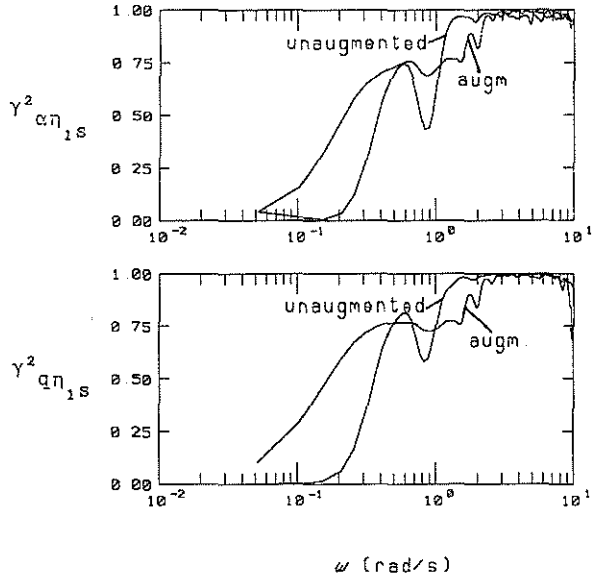

Figure 23 -- Comparison of incidence and pitch rate to longitudinal cyclic coherency function for augmented and unaugmented configurations at 80kn

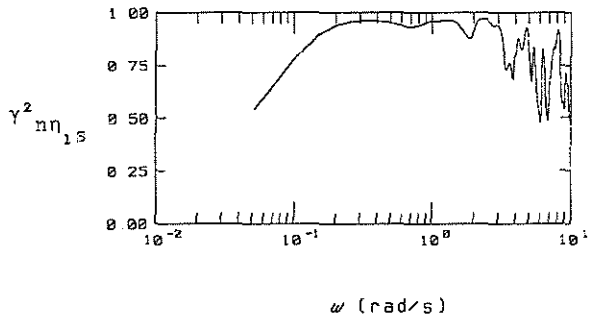

Figure 24 -- Lynx ZD559, flight 115/08/01. Normal acceleration to longitudinal cyclic coherency function

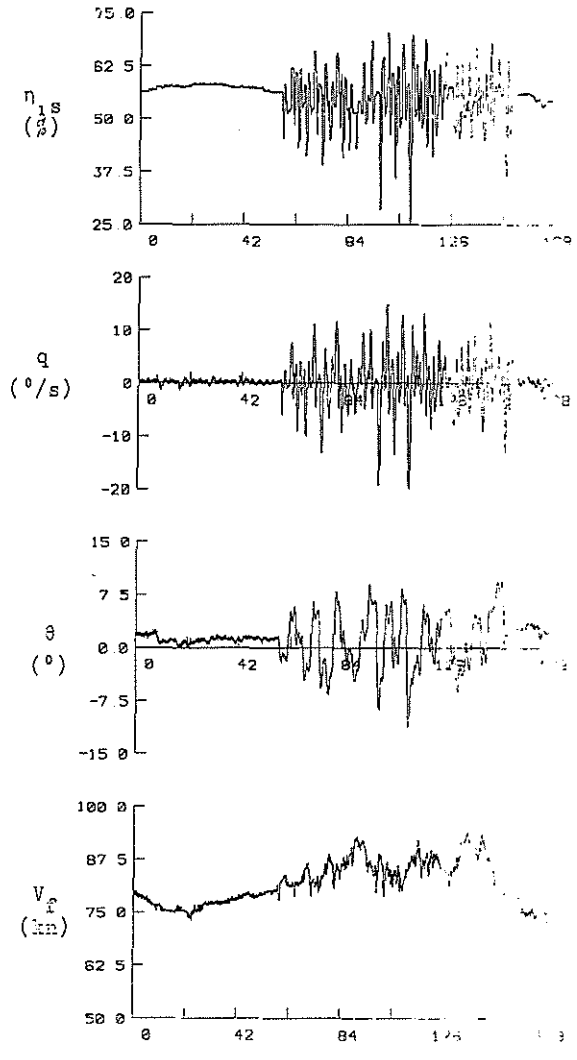

Figure 25 -- Puma XW241, 80kn. Time histories of control input and response during tracking experiment - augmentation engaged

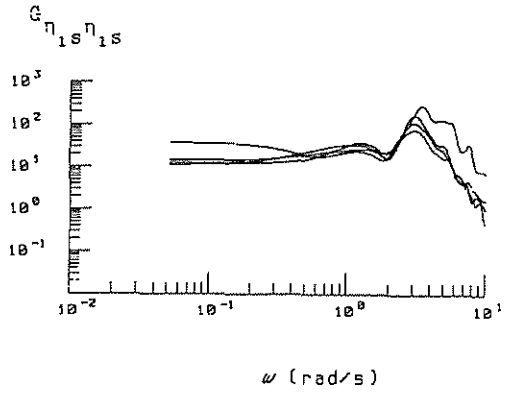

Figure 26 -- Comparison of longitudinal cyclic stick autospectra, all pilots, augmentation engaged, 80kn

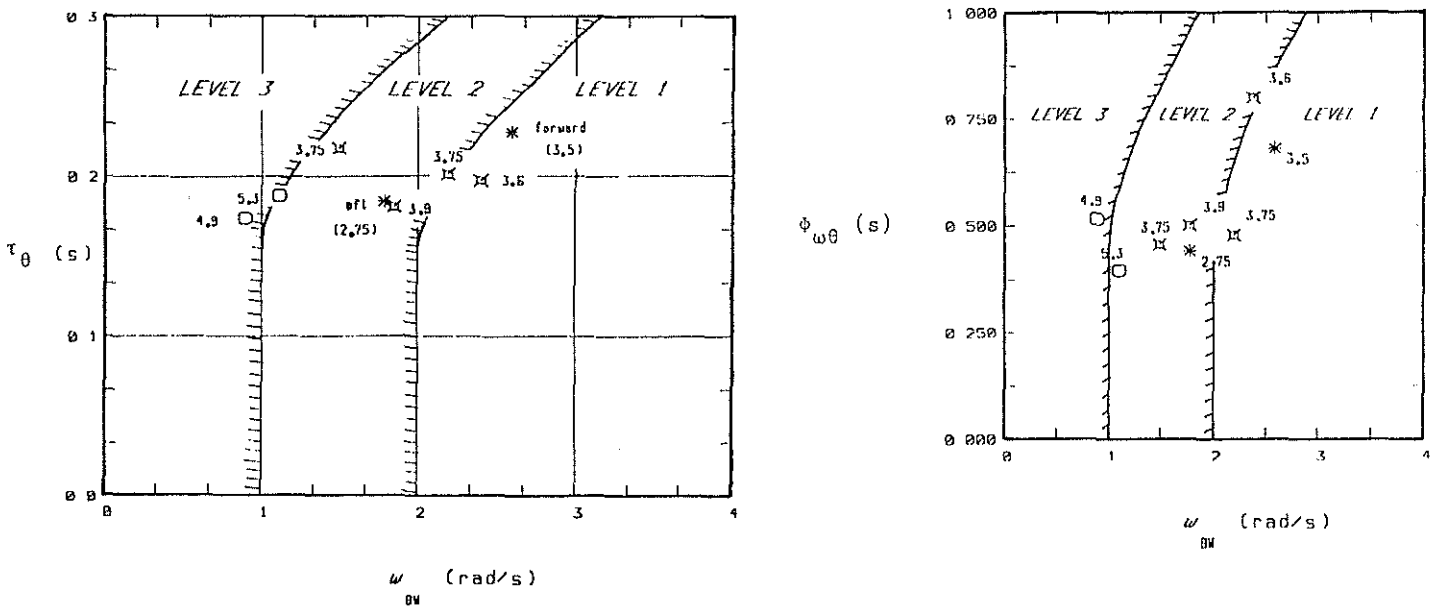

Figure 27 -- Puma characterisation in terms of two bandwidth criteria (a) - delay-bandwidth, (b) - phase slope-bandwidth

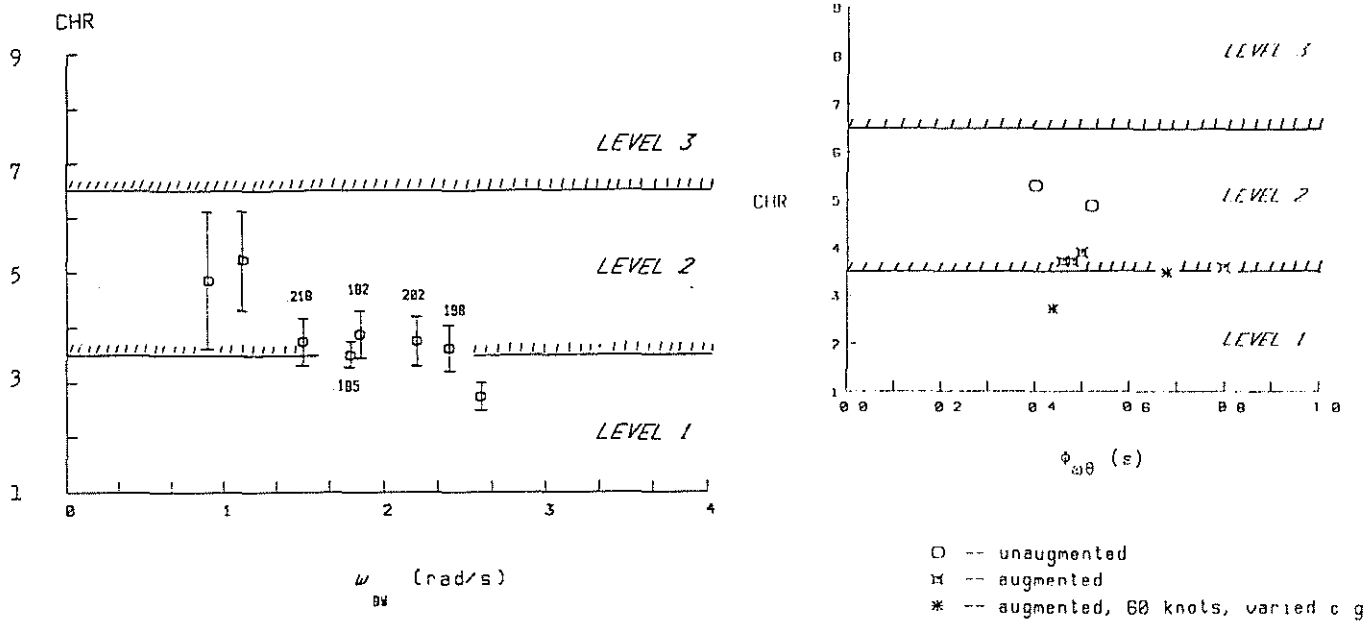

Figure 28 -- Variation in pilot rating with (a) - bandwidth, (b) - phase slope

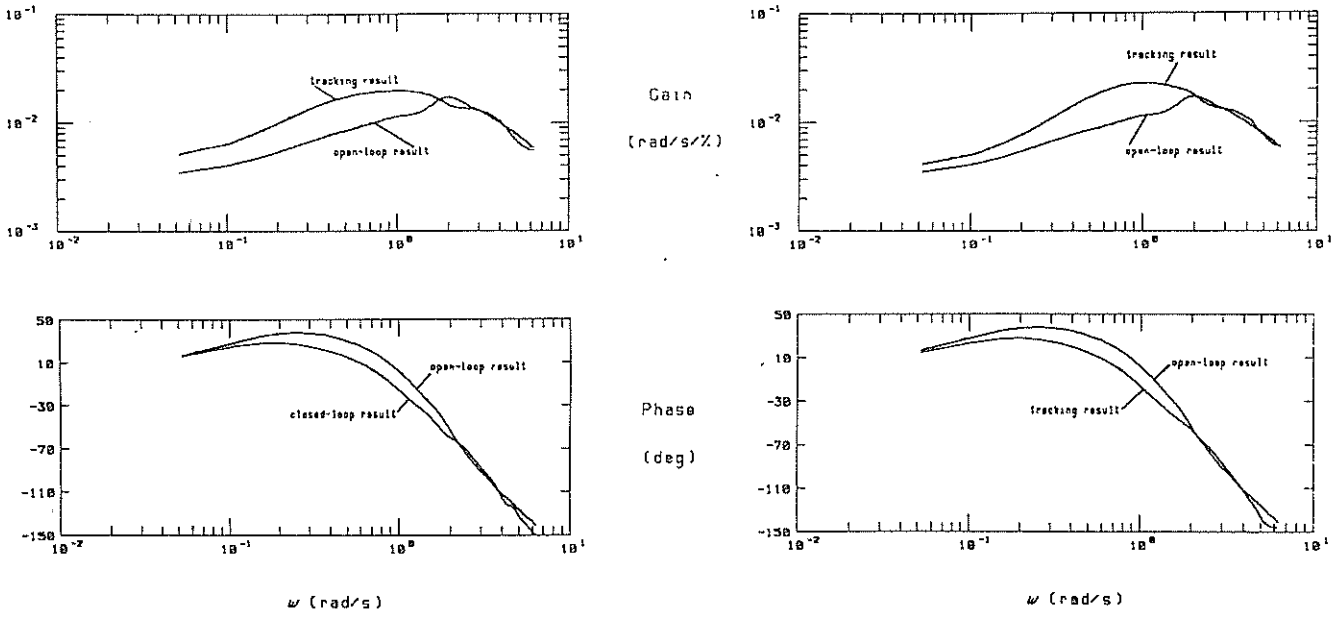

Lt Cdr R Horton, RN Flight 706/05 Airspeed=80 knots, Augmentation engaged in all axes

Maj P Whitfield, AAC Flight 707/03 Airspeed=80 knots, Augmentation engaged in all axes

Figure 29 -- Comparison of open- and closed-loop pitch rate to longitudinal cyclic frequency responses from typical runs.

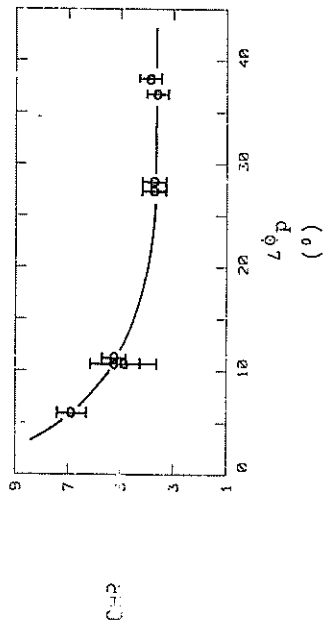

Figure 30 -- Variation in pilot rating with effective phase margin

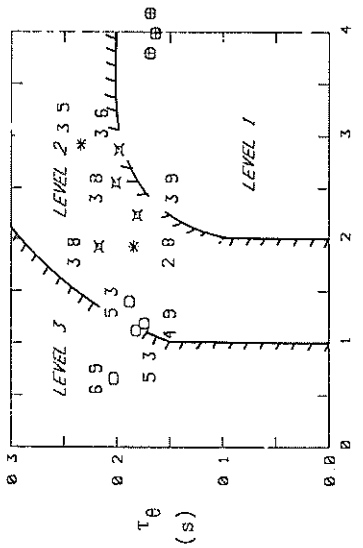

□ -- Puma, unaugmented
✕ -- Puma, augmented
✱ -- Puma, varied c g
⊞ -- Lynx

Figure 31 -- Puma and Lynx pitch axis dynamics characterised by equiv delay and bandwidth (margin=30deg). Modified Level 1 boundary